

Spring 2012

# Detection of trehalose in porphyra extracts using mass spectrometry and gas chromatography-mass spectrometry

Ying Huo

*University of New Hampshire, Durham*

Follow this and additional works at: <https://scholars.unh.edu/thesis>

---

## Recommended Citation

Huo, Ying, "Detection of trehalose in porphyra extracts using mass spectrometry and gas chromatography-mass spectrometry" (2012).  
*Master's Theses and Capstones*. 719.  
<https://scholars.unh.edu/thesis/719>

This Thesis is brought to you for free and open access by the Student Scholarship at University of New Hampshire Scholars' Repository. It has been accepted for inclusion in Master's Theses and Capstones by an authorized administrator of University of New Hampshire Scholars' Repository. For more information, please contact [nicole.hentz@unh.edu](mailto:nicole.hentz@unh.edu).

**DETECTION OF TREHALOSE IN PORPHYRA EXTRACTS  
USING MASS SPECTROMETRY  
AND GAS CHROMATOGRAPHY-MASS SPECTROMETRY**

**BY**

**YING HUO**

**B.S., Jilin University, P.R.China, 2003**

**THESIS**

**Submitted to the University of New Hampshire  
Partial Fulfillment of  
The Requirement for the Degree of**

**Master of Science  
In  
Biochemistry**

**May, 2012**

UMI Number: 1518027

All rights reserved

INFORMATION TO ALL USERS

The quality of this reproduction is dependent upon the quality of the copy submitted.

In the unlikely event that the author did not send a complete manuscript and there are missing pages, these will be noted. Also, if material had to be removed, a note will indicate the deletion.

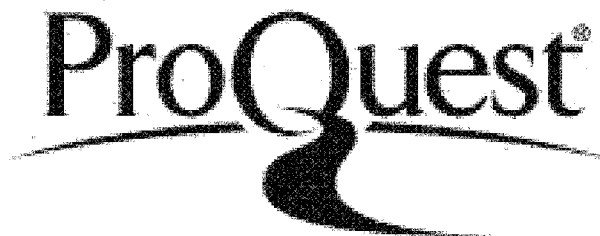


UMI 1518027

Published by ProQuest LLC 2012. Copyright in the Dissertation held by the Author.

Microform Edition © ProQuest LLC.

All rights reserved. This work is protected against unauthorized copying under Title 17, United States Code.



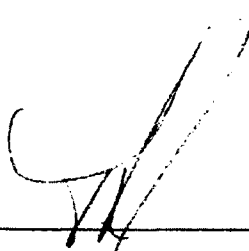
ProQuest LLC  
789 East Eisenhower Parkway  
P.O. Box 1346  
Ann Arbor, MI 48106-1346

This thesis has been examined and approved.



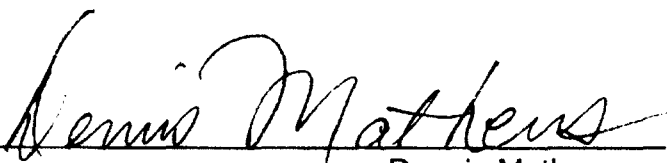
---

Thesis Director, Vernon N. Reinhold,  
Professor of Bio-analytical Chemistry



---

Thomas M. Laue,  
Professor of Biochemistry and Molecular Biology



---

Dennis Mathews,  
Professor of Plant Biology

April 16, 2012

---

Date

## TABLE OF CONTENTS

LIST OF TABLES.....	iv
LIST OF FIGURES.....	v
ABSTRACT.....	ix

CHAPER	PAGE
1. INTRODUCTION	
1.1 Glycans.....	1
1.2 Glycans and Proteins.....	1
1.3 Structural Features of Glycoproteins.....	2
1.4 N-linked Glycans.....	3
1.5 Methods of Glycan Analysis.....	6
2. DETECTION OF TREHALOSE IN PORPHYRA EXTRACTS USING MASS SPECTROMETRY AND GAS CHROMATOGRAPHY-MASS SPECTROMETRY.....	11
2.1 Introduction.....	11
2.2 Experimental section.....	17
2.3 Results and Discussion.....	22
2.4 Conclusion.....	54
REFERENCES.....	55

## LIST OF TABLES

Table 2.1 Characteristic peaks for trehalose in MS <sup>1</sup> .....	23
Table 2.2 major peaks in the MS <sup>2</sup> of ion m/z 477 of permethylated samples: trehalose standard 0.0342µg/µl; fully hydrated Porphyra extracts; fully hydrated Porphyra extracts with trehalose standard 0.0342µg/µl; partially desiccated Porphyra extracts.....	39
Table 2.3 Comparison of characteristic peak retention time on carbohydrate derivative.....	49
Table 2.4 The relation of trehalose derivative characteristic peak area and trehalose quality.....	49
Table 2.5 Comparison of trehalose content between full hydrated and partially desiccated Porphyra extracts.....	54

## LIST OF FIGURES

Figure 1.1 N-linked and O-Linked glycoproteins.....	3
Figure 1.2 Three kinds of N-linked glycoproteins.....	4
Figure 1.3 Electrospray Ionization Ion Trap Mass Spectrometry.....	10
Figure 2.1 Chemical structure of trehalose.....	12
Figure 2.2 Desiccated Porphyra at low tide and Fully hydrated Porphyra at high tide.....	13
Figure 2.3 Scheme for detecting trehalose in Porphyra extracts .....	15
Figure 2.4 MS <sup>1</sup> profiles of trehalose standard 0.0342µg/µl and the blank sample.....	24
Figure 2.5 MS <sup>1</sup> profiles comparison of permethylated samples: trehalose standard 0.0342µg/µl; fully hydrated Porphyra extracts; fully hydrated Porphyra extracts with trehalose standard 0.0342µg/µl added as the internal control; partially desiccated Porphyra extracts .....	26
Figure 2.6 Nomenclature for carbohydrate fragments generally observed under CID .....	27
Figure 2.7 MS <sup>2</sup> of ion m/z 477 of permethylated trehalose standard 0.0342µg/µl.	28
Figure 2.8 MS <sup>3</sup> of ion m/z 477-241 of permethylated trehalose standard 0.0342µg/µl.....	29
Figure 2.9 Fragmentation patterns proposed for the product ions of MS <sup>3</sup> m/z 477-241 of permethylated trehalose standard 0.0342µg/µl.....	30
Figure 2.10 MS <sup>3</sup> of ion m/z 477-259 of permethylated trehalose standard 0.0342µg/µl.....	31

Figure 2.11 Fragmentation patterns proposed for the product ions of MS <sup>3</sup> of ion m/z 477-259 of permethylated trehalose standard 0.0342µg/µl .....	31
Figure 2.12 MS <sup>3</sup> of ion m/z 477-373 of permethylated trehalose standard 0.0342µg/µl.....	33
Figure 2.13 MS <sup>4</sup> of ion m/z 477-373-343 of permethylated trehalose standard 0.0342µg/µl.....	33
Figure 2.14 Fragmentation patterns proposed for the product ions of MS <sup>3</sup> of ion m/z 477-373 of permethylated trehalose standard 0.0342µg/µl .....	34
Figure 2.15 Fragmentation patterns proposed for product ions of MS <sup>4</sup> of ion m/z 477-373-343 of permethylated trehalose standard 0.0342µg/µl.....	35
Figure 2.16 MS <sup>3</sup> of ion m/z 477-403 of permethylated trehalose standard 0.0342µg/µl.....	36
Figure 2.17 Fragmentation patterns proposed for the product ions of MS <sup>3</sup> of ion m/z 477-403 of permethylated trehalose standard 0.0342µg/µl .....	36
Figure 2.18 Fragmentation patterns proposed for permethylated trehalose....	37,38
Figure 2.19 MS <sup>2</sup> of ion m/z 477 of permethylated samples: trehalose standard 0.0342µg/µl; fully hydrated Porphyra extracts; fully hydrated Porphyra extracts with trehalose standard 0.0342µg/µl added as the internal control; partially desiccated Porphyra extracts.....	42
Figure 2.20 MS <sup>3</sup> of ion m/z 477-241 of permethylated samples: trehalose standard 0.0342µg/µl; fully hydrated Porphyra extracts; fully hydrated Porphyra extracts with trehalose standard 0.0342µg/µl added as the internal control; partially desiccated Porphyra extracts.....	43



Figure 2.21 MS<sup>3</sup> of ion m/z 477-259 of permethylated samples: trehalose standard 0.0342µg/µl; fully hydrated Porphyra extracts; fully hydrated Porphyra extracts with trehalose standard 0.0342µg/µl added as the internal control; partially desiccated Porphyra extracts.....44

Figure 2.22 MS<sup>3</sup> of ion m/z 477-373 comparison of permethylated samples: trehalose standard 0.0342µg/µl; fully hydrated Porphyra extracts; fully hydrated Porphyra extracts with trehalose standard 0.0342µg/µl added as the internal control; partially desiccated Porphyra extracts.....45

Figure 2.23 MS<sup>3</sup> of ion m/z 477\_403 of permethylated samples: trehalose standard 0.0342µg/µl; fully hydrated Porphyra extracts; fully hydrated Porphyra extracts with trehalose standard 0.0342µg/µl added as the internal control; partially desiccated Porphyra extracts.....46

Figure 2.24 GC chromatogram of trehalose .....48

Figure 2.25 Standard curve of trehalose quantification using GC; The amount of trehalose was plotted against the characteristic peak area in the GC chromatograms.....50

Figure 2.26 GC chromatograms of the trehalose standard 0.684µg, the fully hydrated Porphyra extracts, the fully hydrated Porphyra extracts with trehalose standard 0.684µg added into it as the internal control and the partially desiccated Porphyra extracts.....52

Figure 2.27 GC/MS comparison of trehalose derivative characteristic peak of the trehalose standard 0.684µg, the fully hydrated Porphyra extracts, the fully hydrated Porphyra extracts with trehalose standard 0.684µg added into it

as the internal control and the partially desiccated Porphyra  
extracts.....53

ABSTRACT

DETECTION OF TREHALOSE IN PORPHYRA EXTRACTS  
USING MASS SPECTROMETRY  
AND GAS CHROMATOGRAPHY-MASS SPECTROMETRY

by

Ying Huo

University of New Hampshire, May 2012

It is known that trehalose helps many plants to survive under desiccated environment<sup>26</sup>. This property of trehalose has also been proposed to explain why Porphyra could survive desiccation when left on dry land for a long period of time<sup>25</sup>. However, after extensive study<sup>25</sup>, effort at identifying trehalose in Porphyra has been unsuccessful, leaving the question of whether trehalose really exists in Porphyra unanswered. In my thesis research, in collaboration with Dr. Anita Klein, I set out to use ion-trap mass spectrometry and gas chromatography coupled with mass spectrometry to identify and quantify the amount of trehalose in Porphyra extracts. Using these techniques, I was able to show for the first time that trehalose definitely exists and the amount decreases as Porphyra goes through desiccation. These results set the stage for further study in the role of trehalose plays in survival under desiccation.

# CHAPTER 1

## INTRODUCTION

### 1.1 Glycans

A living cell utilizes four major biomolecules as constituent building blocks, and a fifth that is a carbohydrate conjugate of two. They are carbohydrates, nucleic acids, lipids and proteins. Among them, carbohydrates are the most abundant, comprising glycosaminoglycans, glycolipids, and glycoproteins. The term glycan refers to carbohydrate residues attached to a protein, and these are of two types, the O-linked and N-linked, which refers to their attachment position on the protein. Glycans expand the protein's function in two ways; indirectly by modulating the proteins physical properties or its conformation or directly by serving as receptors or adhesive components.

### 1.2 Glycans and Proteins

These glycans are covalently attached to a protein primarily through the amino acids asparagine (N-linked) and serine or threonine (O-linked). Such glycoconjugates exhibit numerous functional activities in cell-cell recognition and adhesion, cell migration during development, blood clotting, the immune response, wound healing and many other important biological processes<sup>1</sup>.

Such conjugates are called glycoproteins and found in high abundance on the outside surface of the plasma membrane, in blood and in the extracellular matrix. They are also found in some specific organelles inside cells, for example, the Golgi apparatus. This site is the primary source of glycoprotein processing. But N-glycans are first attached to the protein in the endoplasmic reticulum (ER) before the protein has completed translation. This high mannose glycan moves from the ER to the Golgi where it is processed specifically to the individual needs of the cell. These resultant conjugates are rich in information, forming extremely specific sites for recognition and high-affinity binding by other proteins<sup>1</sup>.

Glycoproteins have been an interesting topic for many years, especially for the last 20 years when biological function was specifically attributed to glycosylation. This attracted interest from scientists around the world. This interest comes from both their abundance in living organisms, and their diverse functions. Glycoproteins play important roles in cell structure as constituents of cell walls and connective tissues. They are also abundant in blood where they serve many basic functions, as for example, blood clotting. Mucus is a glycoprotein and this glycoprotein is critical for the physical properties of all mucosal secretions. The diverse functions of glycoproteins have been attributed to their variable structures.

### **1.3 Structural Features of Glycoproteins**

Structurally, there are two major kinds of conjugate linkages, to N-, and O-linked glycans. Some glycoproteins exhibit both and many have only one linkage types. These glycoproteins are profoundly affected by the number and size of their conjugates. N-links are formed by carbohydrate attached to the nitrogen atom of asparagine (Asn) and it happens in the endoplasmic reticulum, while O-linked glycoprotein are formed by the glycan attached to the protein through the oxygen of serine (Ser) or threonine (Thr) and this also happens in the Golgi apparatus, (Fig. 1.1). The abundance of N-glycans is high in eukaryotes but less common in prokaryotes<sup>2</sup>.

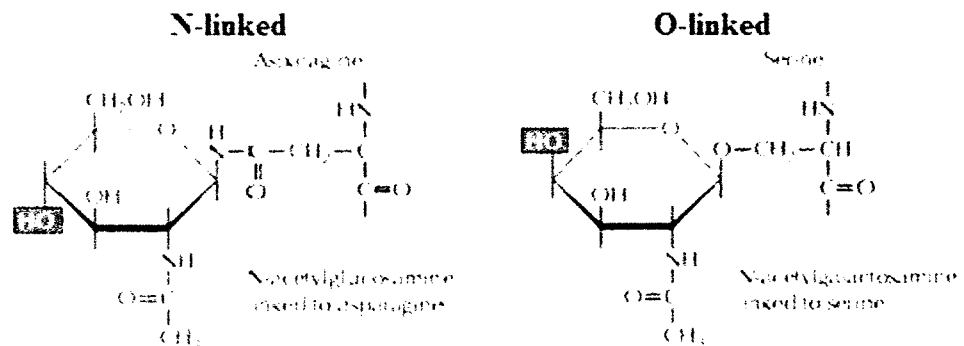


Figure 1.1 N-linked and O-linked glycoproteins

Fig. 1.1 N-linked and O-linked Glycans linked at Amino Acid Sites.

### 1.4 N-linked Glycans

N-linked glycosylation occurs in more than half of the total human proteome. These glycans are attached to asparagine in the sequence Asn-X-Ser or Asn-X-Thr, where X is any amino acid except proline. The glycans are

commonly composed of N-acetylgalactosamine, N-acetylglucosamine, fucose, galactose, mannose and other monosaccharides. All N-glycans share a common pentasaccharide core:  $\text{Man}\alpha 1-6(\text{Man}\alpha 1-3)\text{Man}\beta 1-4\text{GlcNAc}\beta 1-4\text{GlcNAc}\beta 1-\text{Asn}-\text{X-Ser/Thr}^5$ . These N-glycans can be divided into three classes: high-mannose, complex, and hybrid, (Fig.1.2). High-mannose N-glycans (a) have as the common core that is extended with many mannose residues only. For complex N-glycans (b) the core is extended with N-acetylgalactosamine, N-acetylglucosamine, galactose, and frequently fucose (not shown) and often capped with neuraminic acid. The hybrid N-linked glycans (c) represent core extensions of both (a) and (b).

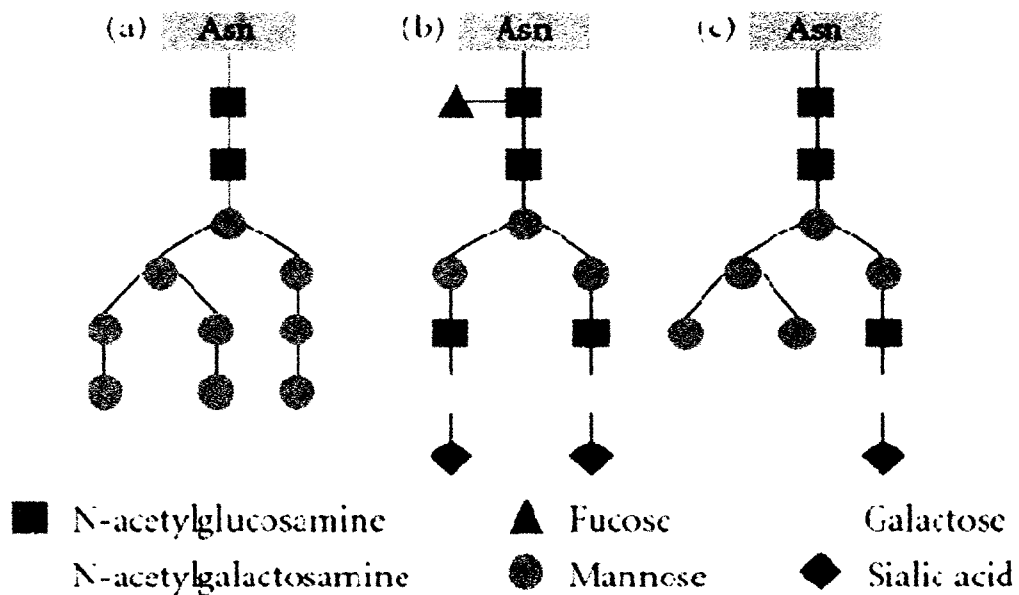


Figure 1.2 Three kinds of N-linked glycoproteins (a) high-mannose (b) complex (c) hybrid

Fig. 1.2 Three kinds of N-linked glycans  
 (a) high-mannose (b) complex (c) hybrid

In eukaryotes, the biosynthesis of N-linked glycans begins from the cytoplasmic face of the endoplasmic reticulum (ER) membrane and ends in Golgi apparatus. Their synthesis occurs in four steps: first, on the external side of the endoplasmic reticulum membrane, a lipid dolichol phosphate conjugates with N-acetylglucosamine in two steps forming Dolichol-P-P-N-acetylglucosamine-N-acetylglucosamine. This precursor is built up with single additions of mannose into an array of three antennae (a, b, c) and finally capped with three glucose residues on antennae c. This structure serves as a precursor for oligosaccharyltransferase which attaches it to the polypeptide chain. The protein-bound N-glycan precursor is now processed by trimming off two of the three terminal glucose residues exposing a single glucose-nine mannose core structure<sup>3</sup>. This important entity binds to cell chaperones that ensure a correct conformation of the peptide. From here the conjugate is processed to a low molecular weight core structure which is extended and modified into two types: complex, and hybrid. These steps are catalyzed by a combination of membrane-bound glycosidases and glycosyltransferases. Some high mannose structures transverse the Golgi unaffected. Defects in N-glycan biosynthesis can cause many kinds of human diseases such as congenital disorders of glycosylation.

In glycoproteins, the attached glycans can directly affect the functions of the conjugated proteins<sup>3</sup>. From *in vivo* studies, it has been reported that changing N-glycans' sialylation and branching can affect erythropoietin's activity<sup>7, 8</sup>. Recent studies also found that N-glycan profiles were changed in disease states and this new or altered glycan structure can influence biological activity in a



negative way<sup>11</sup>. Therefore, the N-glycan profile patterns have been shown to represent disease bio-markers<sup>9, 10</sup>.

N-glycans also play important roles in eukaryotic cells because of the following reasons. First, they facilitate protein folding. It works through the terminal glucose residues and thereby supports protein folding. Additionally, N-linked glycans modulate a protein's structure which is important in cell-cell interactions. Lastly, N-linked glycans are known to target proteins for lysosomal degradation. This is because N-linked glycan are phosphorylated forming a mannose-6-phosphate residue, a marker label for degradation by the lysosome.

### **1.5 Methods of Glycan Analysis**

Although carbohydrates were the first biopolymer identified, our understanding of the biological functions of carbohydrates trails far behind those of proteins and nucleic acids. A large part of the reason for this is our inability to dissect the structural complexity of glycans. Compared with the comprehensive sequencing strategies for both proteins and nucleic acids, a comprehensive strategy for glycan sequencing has been lacking<sup>12</sup>. Glycan analysis is complicated due to the reality that glycans can be branched and joined by a variety of linkages which is the key difference with analysis of nucleic acids and proteins.

Establishing a complete glycan sequence should provide composition, positions of inter-residue linkage, topologies with linear and branching information, stereo and structural isomers, and the sites of glyconjugation.

Glycan structures are usually approached using a variety of methods: which may include, partial enzymatic or acid hydrolysis, which can provide smaller pieces to separate using chromatography. Smaller fragments can be considered for further study by instrumental analyses, like NMR and MS. Another common consideration has been linkage composition analysis as permethylated alditol acetates (PMAA)<sup>3</sup>.

### **High-resolution NMR Spectroscopy**

Glycan analysis depends increasingly on high-resolution NMR spectroscopy. High-resolution NMR spectroscopy is one of the most useful tools for *de novo* glycan characterization<sup>13</sup>. However, the practical use of NMR is limited because of the requirement of relatively large amounts of pure sample needed, , the limitations imposed by molecular weight and sensitivity, as well as the factors that limit their use, such as the instrumental cost and complexity of spectra interpretation.

### **High-performance Liquid Chromatography and Gas Chromatography**

High-performance liquid chromatography and gas-liquid chromatography have also been widely used in analyzing carbohydrate samples. Their strength is that they are good at determining types and amounts of monosaccharide. Their weakness is that it is hard to get information about positions of inter-residue linkage, topologies with linear and branching information and the sites of glyconjugation.

## **Mass Spectrometry**

Mass spectrometry has increasing popularity in analyzing glycan structures because of its high sensitivity and the requirement of relatively small amount of pure samples.

## **MALDI Mass Spectrometry**

Matrix-assisted laser desorption/ionization mass spectrometry (MALDI MS) is a very sensitive tool for determining the mass of the molecular ion to get the composition of the entire oligosaccharide chain; especially the software “GlycoMod” that is used to suggest a “cartoon” structure from the ion composition. GlycoMod is online and free, and easy to use. The shortcoming of MALDI MS is that it cannot get the detailed branching and linking information of the glycan.

## **Tandem Mass Spectrometry**

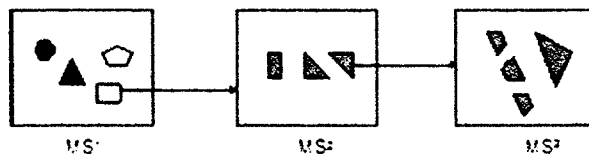
Tandem Mass Spectrometry (MS/MS) has also been used in sequencing glycans. It is good at detecting the mass of the molecular ions and some of its fragments that are result from breakage of the glycosidic bonds<sup>1</sup>. The weakness is that the MS/MS spectra are deficient in terms of assigning the exact details of a carbohydrate<sup>12</sup>.

## **Ion Trap Sequential Mass Spectrometry (MS<sup>n</sup>)**

A method called “Ion Trap Sequential Mass Spectrometry ( $MS^n$ )” has been utilized at University of New Hampshire with a set of software to interpret the  $MS^n$  spectra<sup>14, 15</sup>. Ion trapping MS allows for repeated isolation, fragmentation, and detection of ions, making it possible to reconstruct the detailed structure of a glycan molecule from the successively obtained ion fragments (Fig. 1.3). It works in a procedure as described below: first, a full mass spectrum is obtained called  $MS^1$ ; second, an ion within the  $MS^1$  spectrum, can be selected for further detail fragmented again; the ion is isolated, and all other ions are depleted from the trap. The single isolated ion is now fragmented by a combination of collisional activation with a neutral gas (CID) and pulse electrical activation, in the gas phase of mass spectrometer. The product spectrum obtained from this procedure is called  $MS^2$ . This step can be repeated again ( $MS^{3, 4, 5\dots}$ ), until the ion under study is understood. Spectra from successive fragmentation steps are called  $MS^n$ . Third, the spectral interpretation is assisted by a set of software tools<sup>16, 17</sup>. From multiple  $MS^n$  pathways, and comparing with structural library standards, the components of glycan linkage and branching structures can be assigned.

A method called “Ion Trap Sequential Mass Spectrometry ( $MS^n$ )” has been utilized at University of New Hampshire with a set of software to interpret the  $MS^n$  spectra<sup>14, 15</sup>. Ion trapping MS allows for repeated isolation, fragmentation, and detection of ions, making it possible to reconstruct the detailed structure of a glycan molecule from the successively obtained ion fragments (Fig. 1.3). It works in a procedure as described below: first, a full mass spectrum is obtained called  $MS^1$ ; second, an ion within the  $MS^1$  spectrum, can be selected for further detail fragmented again; the ion is isolated, and all other ions are depleted from the trap. The single isolated ion is now fragmented by a combination of collisional activation with a neutral gas (CID) and pulse electrical activation, in the gas phase of mass spectrometer. The product spectrum obtained from this procedure is called  $MS^2$ . This step can be repeated again ( $MS^{3, 4, 5\dots}$ ), until the ion under study is understood. Spectra from successive fragmentation steps are called  $MS^n$ . Third, the spectral interpretation is assisted by a set of software tools<sup>16, 17</sup>. From multiple  $MS^n$  pathways, and comparing with structural library standards, the components of glycan linkage and branching structures can be assigned.

## Electrospray Ionization Ion Trap Mass Spectrometry



Ion trap allows for repeated isolation, fragmentation, and detection of ions, making it possible to reconstruct the detailed structure of a glycan molecule from the successively obtained ion fragments.

V. N. Reinhold et al. *Methods Enzymol.* 1998, 271, 377-402.

**Figure 1.3** Electrospray Ionization Ion Trap Mass Spectrometry

# **DETECTION OF TREHALOSE IN PORPHYRA EXTRACTS USING MASS SPECTROMETRY AND GAS CHROMATOGRAPHY-MASS SPECTROMETRY**

## **2.1 Introduction**

Porphyra belongs to the phylum of red algae and comprises about seventy species<sup>18</sup>. It grows in intertidal areas, usually between the higher intertidal zone and the splash area in cold waters of temperate oceans<sup>19</sup>. It is the most popular consumable seaweed, which makes it the most domesticated species of aquatic algae<sup>20, 21</sup>. One of the most famous usages of Porphyra is that it is used to wrap fish and rice to make the Japanese food “sushi”. For this reason, it is also an economically important plant species. For example, in Japan alone, the annual production of Porphyra is about one billion dollars<sup>22</sup>.

Trehalose is a unique disaccharide because it is formed through  $\alpha, \alpha$ -1, 1-glucoside bond between two  $\alpha$ -glucose units which makes it a nonreducing disaccharide (Fig. 2.1). Trehalose is synthesized by fungi, plants, and invertebrate animals<sup>23</sup>. Trehalose is widely used in many fields because of its stability, water absorbency, and radicalization resistance. Especially in recent years, because of the growing appreciation of the important biological functions of trehalose, it has become one of the most abundant saccharides used in the world of cosmetics and pharmaceuticals.

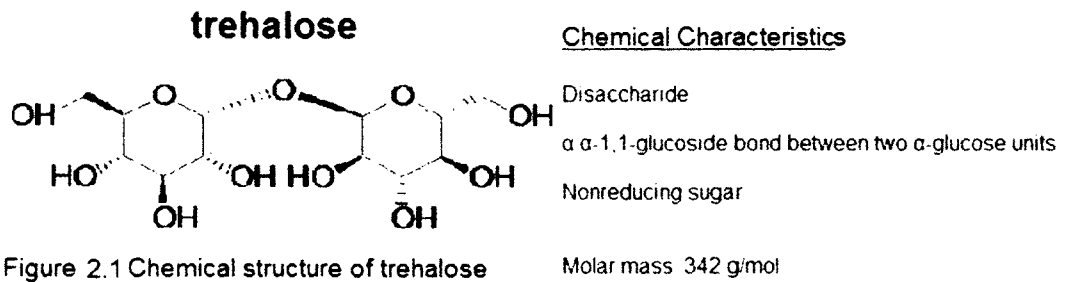


Fig. 2.1 Chemical structure of trehalose

It has been reported that trehalose has roles in helping plants survive in desiccated environments. Consider the *Selaginella* species for example, which spreads in the desert. Even though it may be dried out due to the lack of water for a long time, it will essentially revive after a rain. This is thought to be because of the presence of trehalose<sup>24</sup> in this plant. There are two prevalent theories to explain how trehalose helps plants survive desiccation. One is the vitrification theory which explains that trehalose can form a glass-like state under dry conditions that contributes to the preservation of cellular structure<sup>25, 26</sup>. The other is the water displacement theory, whereby during desiccation trehalose may bind to macromolecules and membranes by replacing water and maintaining basic cellular structure<sup>24, 25</sup>. It is believed that a combination of the two theories is at work.

In recent years, an interesting biological question about *Porphyra*'s life cycle links *Porphyra* to trehalose by scientists studying seaweed<sup>25</sup>. The question is how *Porphyra* can survive desiccation during low tide period. According to the knowledge of geography, most places in the ocean usually experience two high tides and two low tides each day<sup>30,31</sup>. As *Porphyra* grows in the intertidal area, it



is exposed to a dry environment during the low tide period for hours every day. What are the essential components that help *Porphyra* survive desiccation and revive after high tide returns has become an interesting question (Fig. 2.2). It was hypothesized<sup>25</sup> that it may be trehalose that helps *Porphyra* survive the desiccation during the low tide period. This hypothesis is based on the following evidence; first, in many plants, it is known that trehalose helps them survive in desiccated environments<sup>26, 27</sup>; second, trehalose has been widely found in red algae species<sup>28</sup>, even though not reported in *Porphyra*<sup>25</sup>; third, genomic data suggests that *Porphyra* contains genes<sup>29</sup> that synthesize trehalose. Therefore it was hypothesized that trehalose may exist in *Porphyra* and help it survive during the long low tide period<sup>25</sup>.

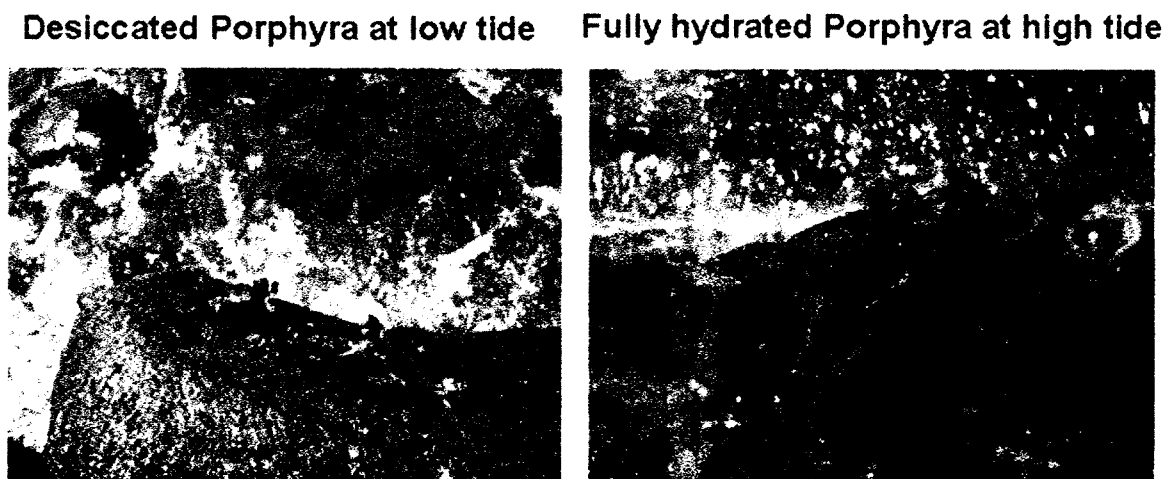


Figure 2.2 Desiccated *Porphyra* at low tide and Fully hydrated *Porphyra* at high tide

Fig. 2.2 Desiccated *Porphyra* at low and fully hydrated *Porphyra* at high tide.

In order to test this hypothesis, carbohydrate screening using NMR and quantification using HPLC has been applied. But the data showed that trehalose

could not be detected in *Porphyra* using these two methods<sup>25</sup>. It is not clear why these instrumental approaches have proved unsuccessful.

In collaboration with Dr. Klein, who is an expert of seaweed research, we are trying to solve the probability of trehalose in *Porphyra* extracts using mass spectrometry and gas chromatography. There are two questions we are interested in. The first one is a qualitative question: whether trehalose can be detected in *Porphyra* extracts using mass spectrometry; the second one is a quantitative question: whether the amounts of trehalose are the same in hydrated and desiccated *Porphyra* samples.

Mass spectrometry has been predominantly used in analyzing glycan structures because of its high sensitivity and the requirement of relatively small amount of pure sample. The method of Ion Trap Sequential Mass Spectrometry ( $MS^n$ ) has been successfully used in analyzing glycan structures through constructing multiple  $MS^n$  pathways<sup>11, 14, and 17</sup>. This would be the first time that mass spectrometry has been applied in detecting trehalose. The commercial value of *Porphyra* will dramatically increase if trehalose is found in *Porphyra* to help with desiccation and this would definitely improve *Porphyra*'s prosperity of industrialization.

Gas chromatography is good at determining types and amounts of monosaccharides, which has made it a powerful tool for quantification and it has been routinely used in detecting and quantifying trehalose<sup>39</sup> in many other plants<sup>32</sup>. This will be the first time that gas chromatography is used in comparing the amount of trehalose between hydrated and desiccated *Porphyra* samples.

This will also facilitate our understanding of the mechanism of how trehalose helps plants survive in a desiccation environment.

To characterize trehalose an experimental approach was designed as shown, (Fig. 2.3). Samples were first purified using porous graphitized carbons (PGC). The samples were then separated into two batches. One batch was treated by permethylation and then injected into mass spectrometer to check if there was trehalose in *Porphyra* extracts; the other batch was treated with Tri-Sil HTP (TMS) reagent to obtain TMS derivatization and then injected into gas chromatography to check if there was trehalose in the *Porphyra* samples and the amount of trehalose in hydrated and desiccated *Porphyra* samples.

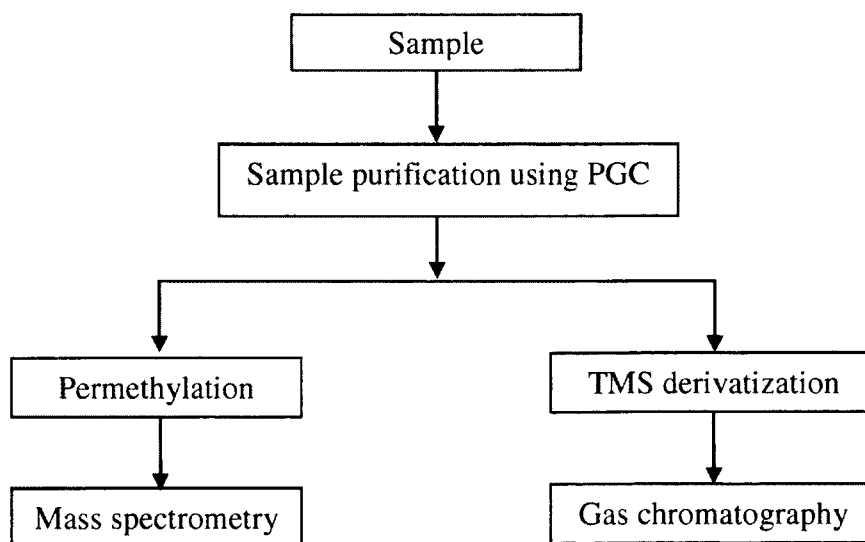


Fig. 2.3 Scheme for detecting trehalose in *Porphyra* extracts

Permethylation is an important strategy for oligosaccharide structural characterization for the following reasons: first, permethylation can locate

glycosidic bonds; second, it can enhance ion signals<sup>33, 34</sup>. Trimethylsilation is a necessary step of gas chromatography sample preparation because the sample needs to be volatilized for chromatography and subsequently resolved and detected.

## **2.2 Experimental Section**

### **Materials and Reagents**

Porphyra extracts and the sample preparation protocol were provided by Dr. Klein's lab, University of New Hampshire. All of the rest of materials and reagents were of analytical purity and used as received. HPLC grade water, acetonitrile (ACN), and chloroform were purchased from Fisher Scientific (Fairlawn, NJ, USA). Porous graphitized carbon (PGC) was purchased from Alltech Associates (Deerfield, IL). Sodium hydroxide (NaOH), trifluoroacetic acid (TFA), HPLC grade dimethylsulfoxide (DMSO), sucrose and sodium hydroxide (NaOH) beads were obtained from Sigma-Aldrich (St. Louis, MO, USA). Spin Columns were obtained from Harvard Apparatus (Holliston, MA, USA). Methyl iodide (CH<sub>3</sub>I) was received from EM Science (Gibbstown, NJ, USA). Tri-Sil HTP (HDMS: TMSC: pyridine) Reagent was purchased from Thermo Scientific (Bellefonte, PA, USA). Trehalose standard was purchased from Ferro Pfanstiehl Laboratories, Inc (Waukegan, IL, USA).

### **Porphyra extracts preparation**

Porphyra species samples were collected from Ft. Stark, Newington, NH. These samples were then kept in salt water obtained from Dover Point in a tank with a bubbler until use. The salt water tank was contained in a larger tank with circulating cold water. 1.5 hours before samples were taken, individual Porphyra plants were removed from the salt water and placed on a clean surface

to experience a "low tide" partially dehydrated state. The Porphyra was then removed from the tank, patted dry on a paper towel, and cleaned on each side using a Q-tip. Cleaned plant samples were then ground to a fine powder in liquid N<sub>2</sub>. 30 mg of this powder was measured into 1.5 mL microcentrifuge tubes and 200 µL of water were added. Each sample was thoroughly vortexed and subsequently centrifuged at 16000rpm for 1 minute. Supernatant (100 µL) was then transferred to a clean microcentrifuge tube. Hydrated samples followed same protocol but did not have the 1.5 hour "low tide" treatment.

### **Sample purification using PGC**

Dried out samples were purified by using a PGC column. PGC purification of glycans was carried out as below. Firstly, PGC was prewashed 3 times with 1 M NaOH, 1 time with water, 1 time with 80% ACN/ 20% water in 0.1% TFA, 1 time with 75% ACN/25% water in 0.1% TFA and the PGC packed column was equilibrated with 4 mL of water. Secondly, samples were applied into the PGC column and eluted by 5 aliquots of 1 mL of water. Thirdly, the 5 mL eluent was dried out in a Speedvac.

### **Permethylation**

Spin Column was washed twice by 0.3 mL DMSO before adding NaOH beads and then the column was packed with about 3cm of NaOH beads. NaOH beads were washed with DMSO twice. Glycan sample was suspended in 60 µL DMSO, 45 µL MeI and 2 µL water and applied to the spin column. A red cap was

gently placed on the column and the column was incubated at room temperature for 15 minutes. The column was centrifuged for 60 sec at the speed of 2000 rpm. 45  $\mu$ L MeI was added to the flow through and all the material at the bottom of the column was applied back to the spin column and centrifuged for 60 sec at the speed of 2000 rpm. The flow through was added with 100  $\mu$ L ACN and spun for 60 sec at 2000 rpm. Liquid/Liquid extraction was performed with Chloroform 5 times and each time by adding 1.5 mL chloroform and 3 mL H<sub>2</sub>O. Samples were dried out in a SpeedVac.

#### **Preparation of the TMS derivatives**

Dried samples were treated by adding 200  $\mu$ L of Tri-Sil HTP reagent into each reaction and then placed on heat block at 80°C for 20 minutes. Samples were cooled rapidly to room temperature and evaporated just to dryness under a stream of nitrogen gas at room temperature. Samples were dissolved in 1 mL of chloroform, vortexed, centrifuged and then the top 850 $\mu$ L was removed and saved in a separate new tube. This step was repeated twice and the top supernatants were combined. Samples in the new tube were dried in a SpeedVac until dry. 100 $\mu$ L of chloroform was added into each sample and 3  $\mu$ L was injected into the GC-MS system.

#### **Separation of the TMS derivatives using GC/MS**

The equipment we used was Finnigan PolarisQ GC/MS Benchtop Ion Trap Mass Spectrometer of Thermo Electron Corporation (Austin, TX, USA),

supplied with ion trap detection (ITD) system and a TriPlus autosampler (Austin, TX, USA). The column used was the product of Agilent Technologies (New Castle, Delaware, USA); code: DB-5MS, 30m× 0.25mm× 25µm.

The temperature program for gas chromatography was set as below:

Injections were made at 200°C, held at 200°C for 0.5 minute, and then elevated to 300 °C with the ramp 10°C/min and held at 300°C for 10min.

The temperature of the transfer line was 260°C. The actual parameters of the ITD system were defined by the automatic set up mode.

The actual ITD parameters were: mass range: 50-650 Dalton; ionization mode: EI; ionizing potential: 70eV; filament emission current: 250µA; s/scan: 25; Fil/Mul delay 4min; peak threshold 0 count.

### **ESI Mass Spectrometry and Data Interpretation**

Mass spectra were obtained using a LTQ, an MS<sup>n</sup> mass spectrometer (Thermo Fisher Scientific, Waltham, MA). This instrument was equipped with a TriVersa Nanomate (Advion) automated ion injection source. Samples were infused at flow rates ranging from 0.30 to 0.60 µL/min. Spectra were collected by using Xcalibur 1.4 and 2.0# software (Thermo Fisher Scientific). Average signal was accomplished by 5 micro-scans within each scan and adjusted 50 to 300 scans in each spectrum depending on signal intensity. This improved spectral quality and was important, especially at the higher orders of MS<sup>n</sup>, particularly beyond MS<sup>5</sup> or MS<sup>6</sup>. Normalized collision energy was set at 35%; activation Q was set at 0.25 and activation time for 30 ms. The relative abundance of product



ions cannot be affected by changing the collision energy, but the abundance of precursor ion can. Activation time and the activation Q were kept constant because the product ion abundances can be influenced by them.

In-house bioinformatics tools developed by Hailong Zhang were used to assist data analysis. Ion trapping allows for repeated isolation, fragmentation, and detection of ions, providing fragments to reconstruct the detailed structure of a glycan molecule from the successively obtained ion fragments. It works in a procedure as described below: first, after the sample is injected into the mass spectrometer, the full mass spectrum is obtained and this is called  $MS^1$ ; second, an ion of interest the spectra is selected as precursor ion and can be fragmented again. In this step, the selected precursor ion is isolated to a alternative trajectory and the remaining ions ejected. Secondly, a collision gas is introduced (CID) to obtain additional structural detail on the isolated fragment. The spectrum obtained from this procedure is called  $MS^2$ . This step can be repeated again and again until the most detailed structure is obtained. The spectrum from the successive steps is called  $MS^n$ . Third, the spectral interpretation are assisted using a set of software that provided an understanding of the structural details. From multiple  $MS^n$  pathways, a fragment library of standards, glycan's structure can usually be determined, including interresidue linkage and structural isomers.

## **2.3 Results and Discussion**

In this project, our goal was to answer two questions about trehalose in Porphyra. The first is a qualitative question: whether trehalose is present, and the second, is a quantitative question, how much. Was the amount of trehalose the same in hydrated and desiccated Porphyra samples? In order to present the data clearly, the results are presented as two parts: (1) Mass spectrometry analysis; (2) Gas chromatography-mass spectrometry analysis.

### **Mass spectrometry analysis**

Five samples were processed in parallel and they were: ① the blank sample, as the negative control; ② the trehalose standard 3.42 $\mu$ g; ③ the fully hydrated Porphyra extracts; ④ the fully hydrated Porphyra extracts with trehalose standard 3.42 $\mu$ g added into it as the internal control; ⑤ the partially desiccated Porphyra extracts. All of the samples were purified with PGC first and then permethylated before they were finally injected into Mass Spectrometer for analysis. The permethylated samples were dissolved in 90% methanol, and 10 $\mu$ l was injected into LTQ Mass Spectrometer. The characteristic ion for trehalose in MS<sup>1</sup> profile was observed, m/z 477 (with Na<sup>+</sup> adducted) after permethylation (Table 2.1).

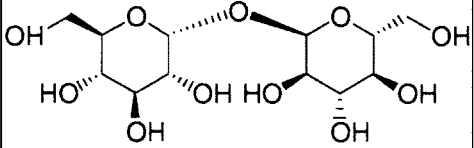
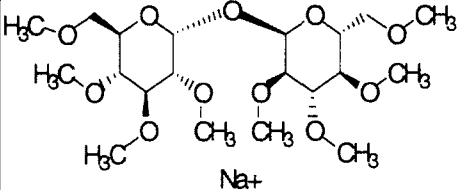
Trehalose	Before Permethylation	After Permethylation
Molecular weight	342	477 (with Na <sup>+</sup> adducted)
Structure		

Table 2.1 Characteristic peaks for trehalose in MS<sup>1</sup>. After permethylation, the molecular weight of trehalose becomes 477, which was ion observed in the trehalose spectrum.

The ion  $m/z$  477 was found in sample ②: trehalose standard  $0.0342\mu\text{g}/\mu\text{l}$  as expected and it was the most abundant peak. All the other minor peaks also appeared in sample ① blank (Fig. 2.4). In order to confirm if the ion was trehalose in the Porphyra samples, further fragmentations was carried out on both the Porphyra samples and the trehalose standard. The results are presented in three sections: (1) MS<sup>1</sup> spectral comparison between the standard and the Porphyra extracts; (2) spectral patterns of trehalose; and (3) spectral comparison of the MS<sup>n</sup> spectra obtained from the ion  $m/z$  477 of the trehalose standard and the Porphyra samples.

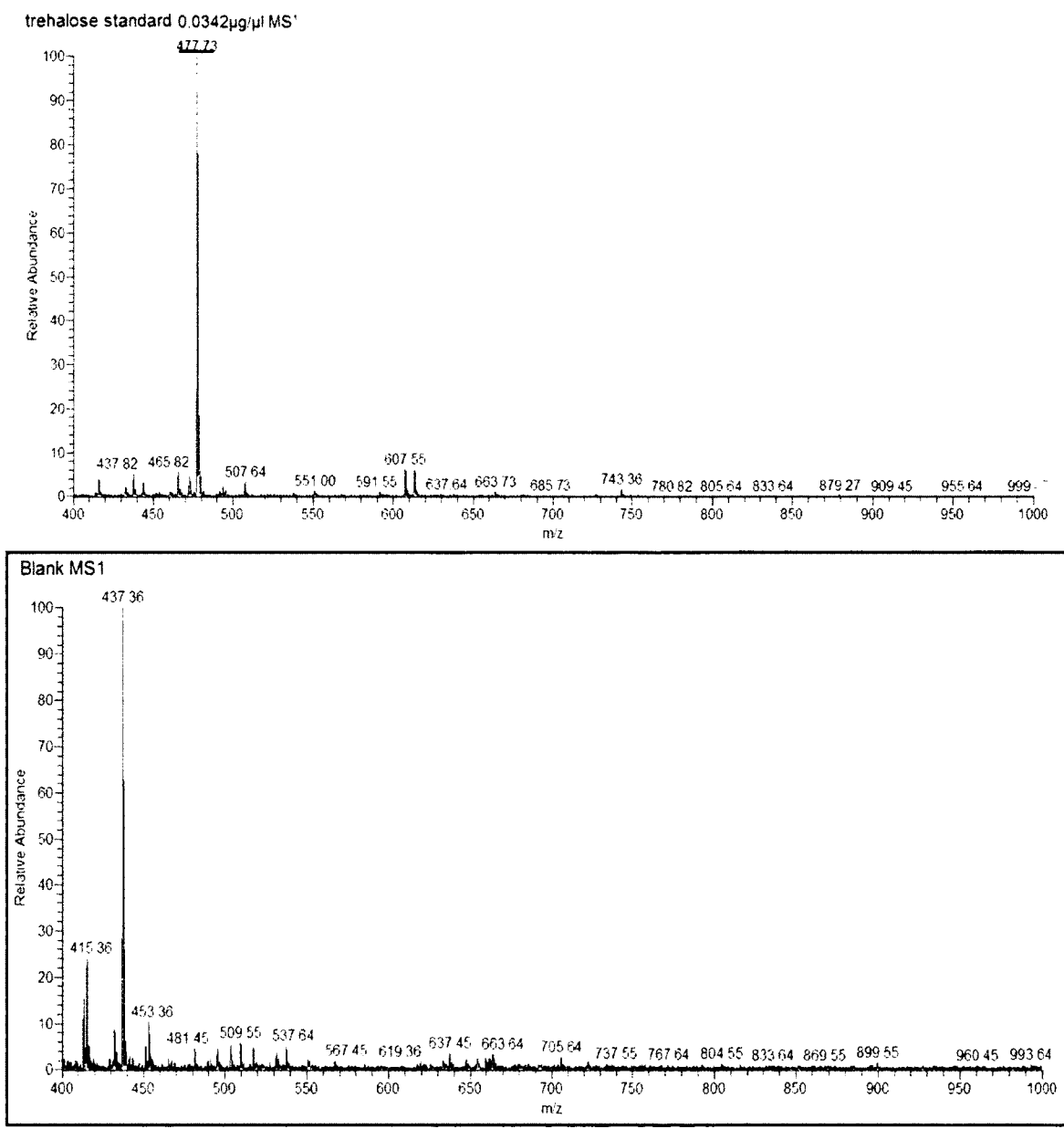


Fig. 2.4 MS<sup>1</sup> profiles of trehalose standard 0.0342µg/µl and the blank. The ion of m/z 477 marked with a red line was observed as the major ion in the MS<sup>1</sup> spectrum of trehalose standard and all the other minor peaks have been found in the MS<sup>1</sup> profile of the blank sample. All spectra are displayed to show the most abundant ion as the base ion.

### **(1) Comparison of MS<sup>1</sup> profiles**

In order to see whether trehalose could be detected in Porphyra extracts, we first compared MS<sup>1</sup> spectra of the Porphyra extracts samples with that of the trehalose standard. The ESI MS profiles from the four samples: the trehalose standard 0.0342µg/µl; the fully hydrated Porphyra extracts; the fully hydrated Porphyra extracts with trehalose standard 0.0342µg/µl added into it as the internal control; and the partially desiccated Porphyra extracts (Fig. 2.5). The MS<sup>1</sup> spectra of the latter three samples have a lot of similarities. The characteristic peak at ion of m/z 477 of the permethylated trehalose was found in the positive control sample and the fully hydrated Porphyra extracts with trehalose standard added as expected, while it has also been found in the MS<sup>1</sup> profiles of the fully hydrated Porphyra extracts and the partially desiccated Porphyra extracts. More importantly, in all four samples, the m/z 477 ion showed up as the major peak. Now the question was whether the m/z 477 ion that showed up in all of the Porphyra extracts samples was due to natural occurring trehalose as it was in the trehalose standard. In order to answer this question, the CID patterns were studied (Fig.2.5).

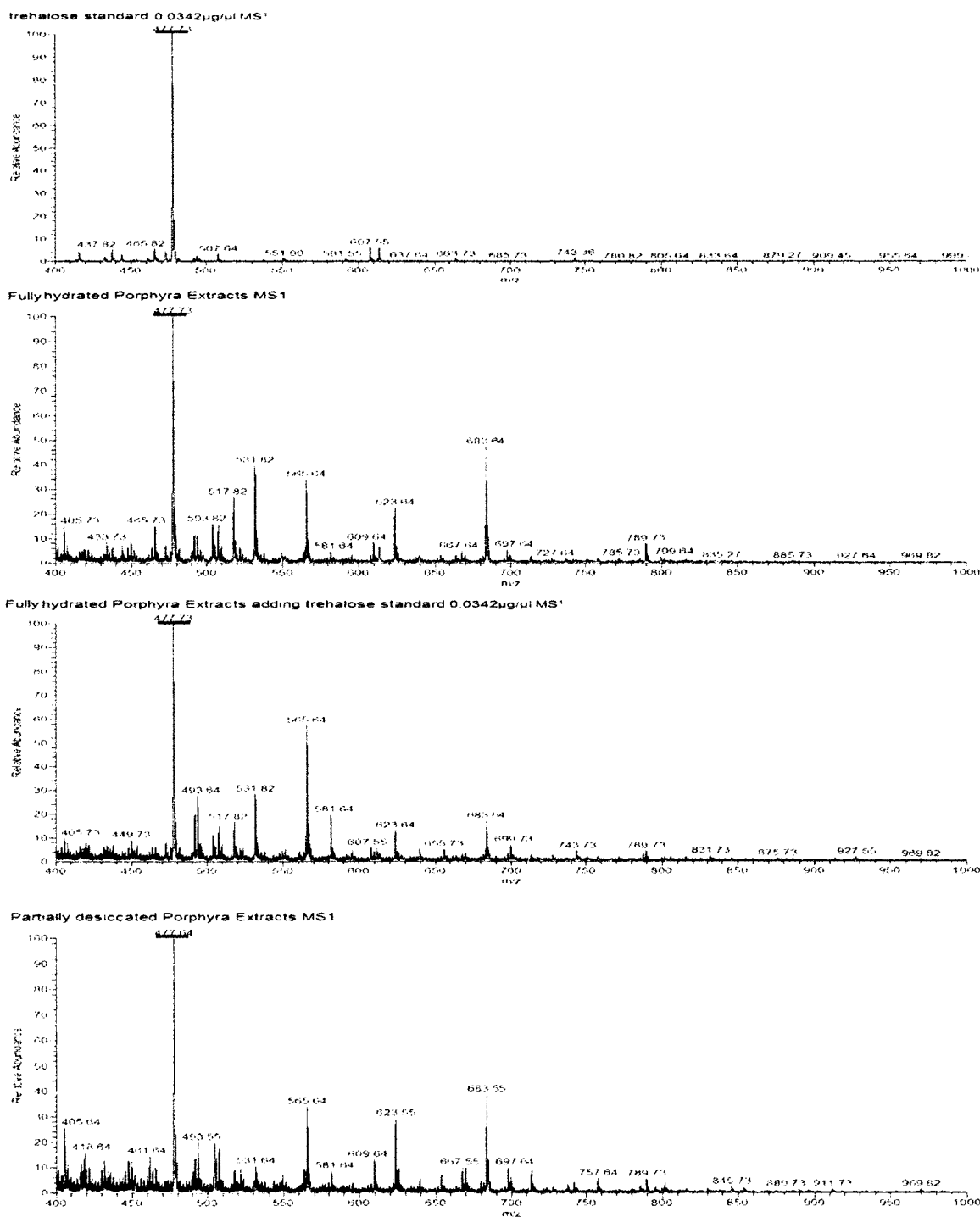


Fig. 2.5 MS<sup>1</sup> profiles of permethylated samples: trehalose standard 0.0342 μg/μl;

fully hydrated Porphyra extracts; fully hydrated Porphyra extracts with trehalose standard 0.0342 $\mu\text{g}/\mu\text{l}$  added as the internal control; partially desiccated Porphyra extracts.

## **(2) Fragmentation patterns of trehalose**

There are two major fragments in glycosidic samples as a result of CID: glycosidic bond and cross-ring cleavages<sup>35</sup>. Glycosidic cleavage is the result of C-O bond rupture providing B- and Y- ions, (Fig. 2.6). Alternatively, rupture could occur on the distal side of the glycosidic oxygen providing C- and Z-type ions, (Fig. 2.6). A cross-ring cleavage ruptures two bonds across the pyran ring of a monomer, which yields A- and X- type ions<sup>5</sup> (Fig. 2.6). Glycosidic cleavages provide monomer connectivity, while cross-ring cleavages provide information of monomer linkage position. For a permethylated sample, glycosidic bond cleavage provides specific pyranosyl-1-ene (B-ion) and Z-type ions with an open hydroxyl (Y-type ion). These cleavage identifiers are called as scars<sup>12</sup>. The position of such scars is determined by the composition mass of the ion under investigation. Generally, facile bond ruptures are mostly glycosidic bonds, B-/Y-type and C-/Z-type. Double cleavage cross-ring product ions are observed more commonly under higher energies or with glycans of smaller size where collision energy dissipation is constrained to fewer oscillators.

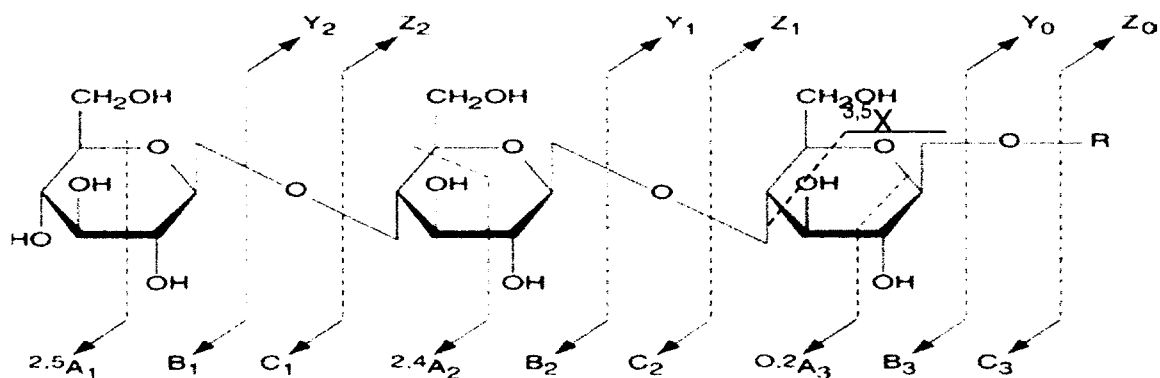


Fig. 2.6 Nomenclature for carbohydrate fragments generally observed under CID

After the MS<sup>1</sup> spectrum has been obtained using the Electrospray ionization ion trap mass spectrometer, the precursor ion m/z 477 was selected and fragmented to confirm its structure (Fig. 2.7). Eight major product ions were observed in this MS<sup>2</sup> spectrum: m/z 227.09, 241.09, 259.09, 329.09, 373.18, 389.18, 403.18 and 445.18. In order to obtain additional structural detail each of these ions, were further selected and collided, MS<sup>3</sup>. As an example, the ion m/z 241.09 was disassembled to provide a detailed structural understanding of this MS<sup>n</sup> process.

trehalose standard 0.0342µg/µl \_MS<sup>2</sup> of peak 477

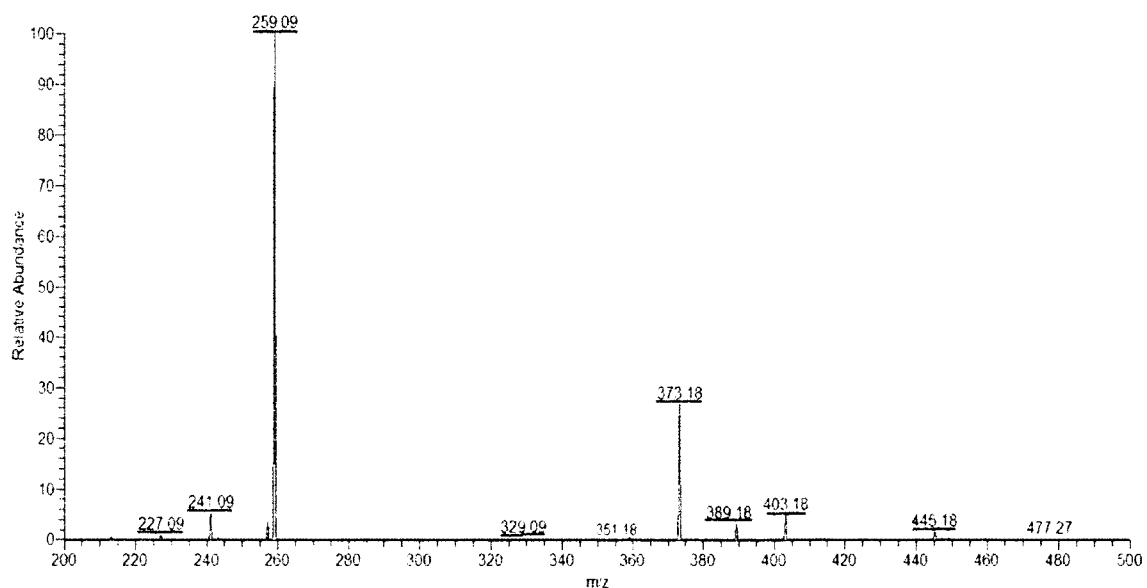


Fig. 2.7 MS<sup>2</sup> of ion m/z 477 of permethylated trehalose standard 0.0342µg/µl

In order to get a more detailed understanding of the ion structure m/z 241.09, further fragmentation was initiated (Fig. 2.8). From this MS<sup>2</sup> spectrum



241.09, four major ions were observed, m/z 139.09, 209.09, 211.09, and 226.09. These products can be explained as showed in Fig. 2.9. Peak m/z 226.09 can be considered a loss of one methyl group, while ions m/z 139.09, 209.09, 211.09 are due to the cleavages shown (Fig. 2.9). From these studies, the structure of ion m/z 241.09 is consistent and expected.

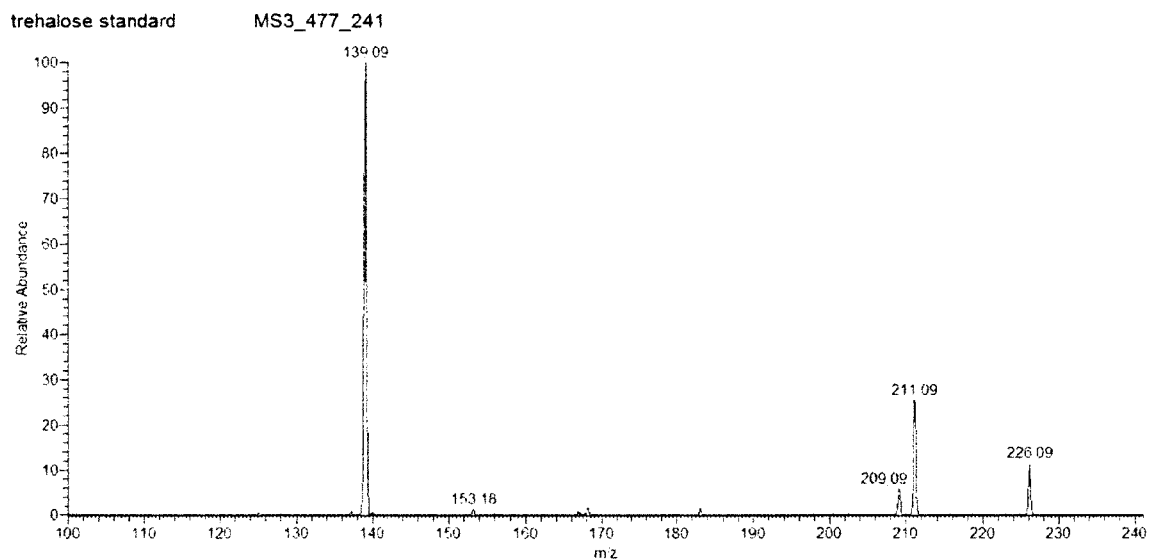


Fig. 2.8 MS<sup>3</sup> of ion m/z 477-241 of permethylated trehalose standard 0.0342µg/µl

MS<sup>2</sup> of the ion with m/z 259.09 (in the spectrum of MS<sup>2</sup> of m/z 477) is also studied using ESI MS (Fig. 2.10). Three major peaks at m/z 155.09, 185.09 and 227.09 were observed. The structure and fragmentation pattern of this m/z 259.09 ion was rationalized (Fig. 2.11).

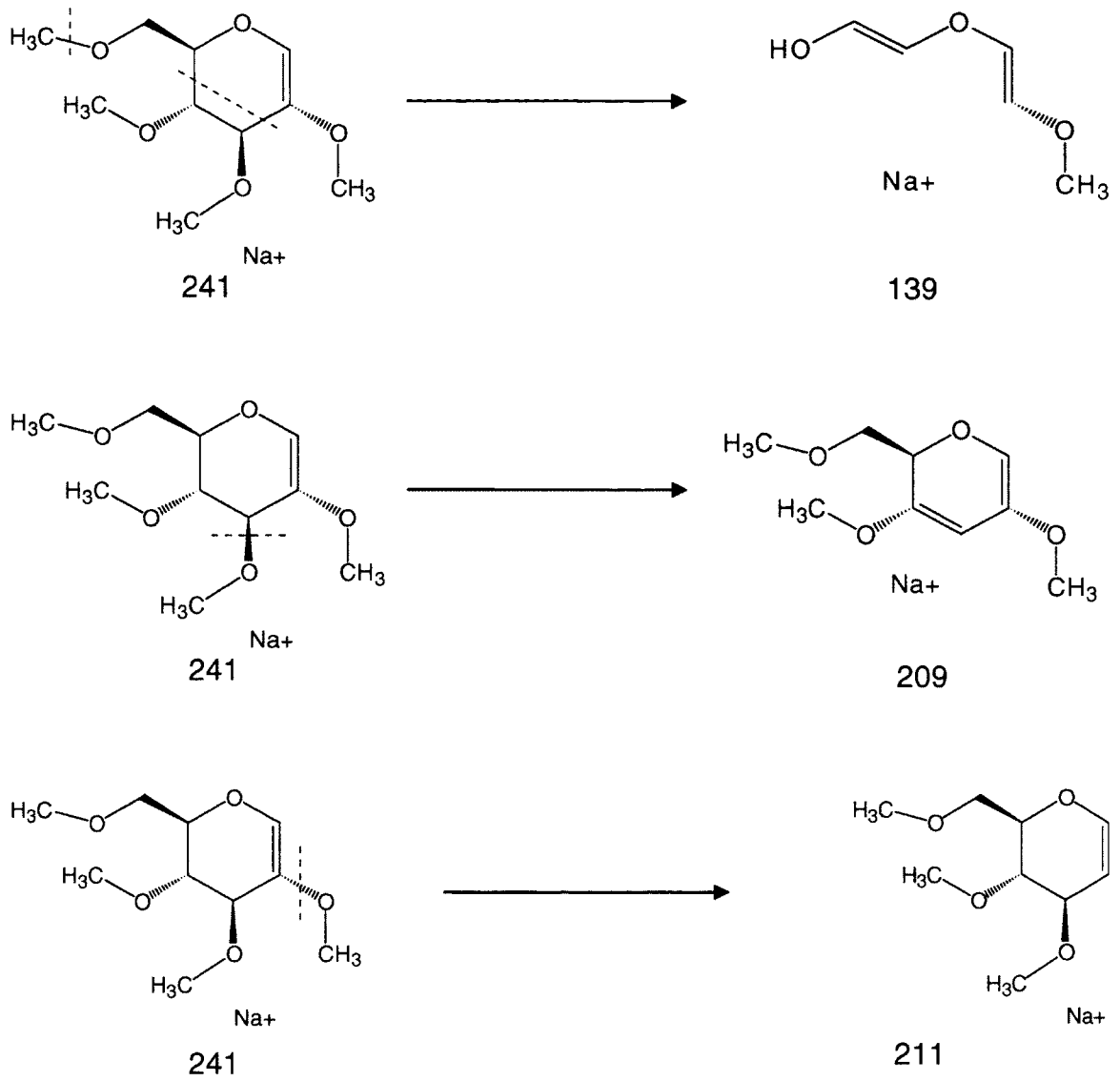


Fig. 2.9 Fragmentation patterns proposed for the product ions of MS<sup>3</sup> m/z 477-241 of permethylated trehalose standard 0.0342 $\mu$ g/ $\mu$ l

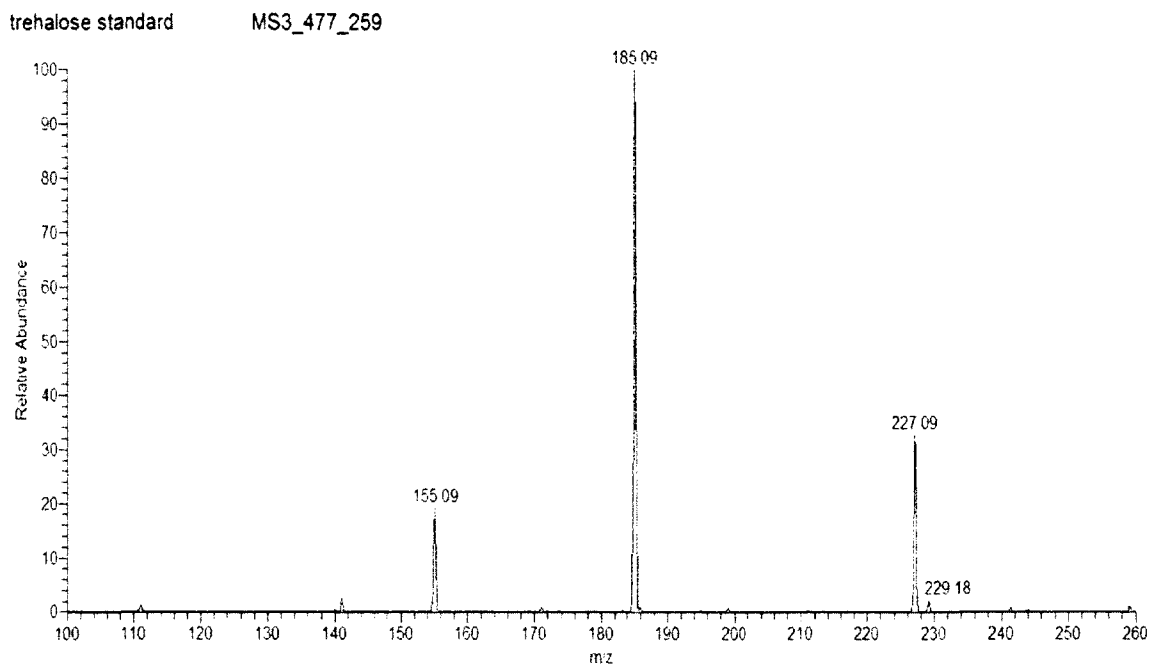


Fig. 2.10 MS<sup>3</sup> m/z 477-259 of permethylated trehalose standard 0.0342μg/μl

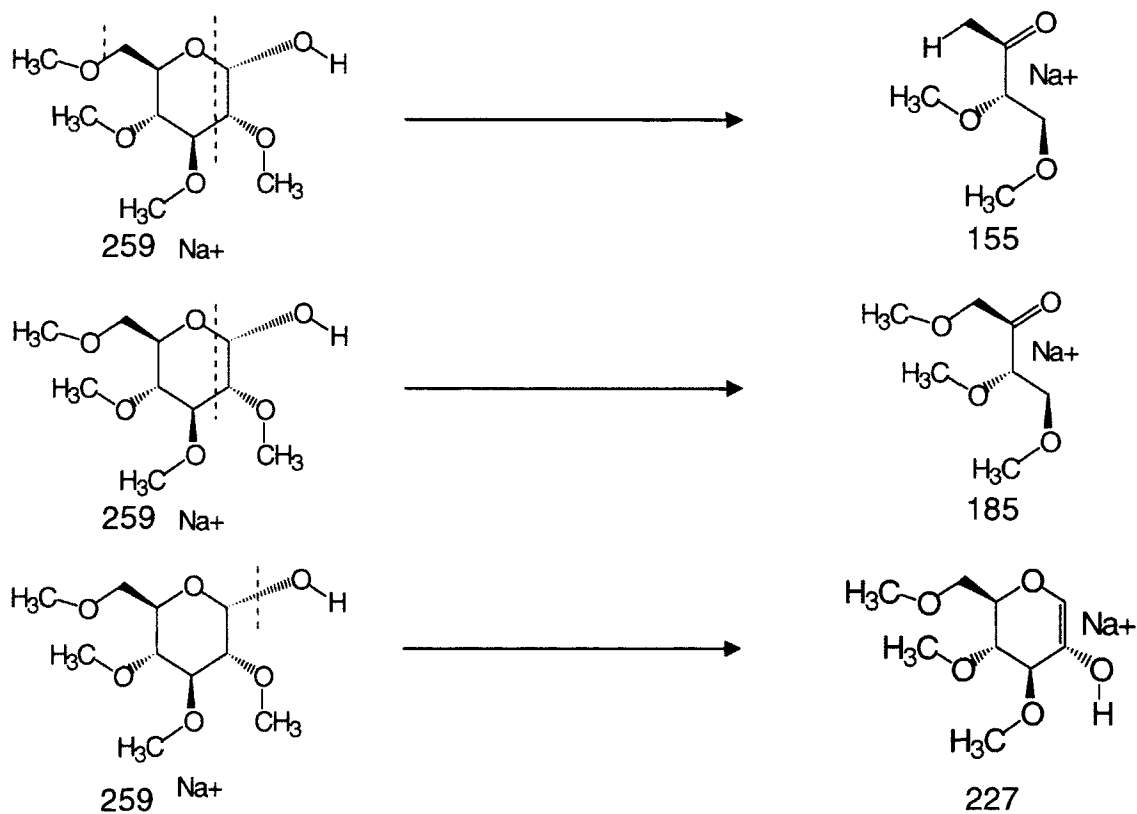


Fig. 2.11 Fragmentation patterns proposed for the product ions of MS<sup>3</sup> m/z 477-259 of permethylated trehalose standard 0.0342μg/μl

In order to get great structural detail, the ion  $m/z$  373.18 ( $MS^2$  477), was disassembled further (Fig. 2.12). From the  $MS^2$  spectrum, three major ions were observed,  $m/z$  257.09, 259.18, and 343.18. The ion with  $m/z$  343.18 is unusual in  $MS^n$  spectra, therefore further fragmentation was pursued (Fig. 2.13). In the  $m/z$  343.18, five major peaks have been found. They are  $m/z$ : 211.09, 241.09, 259.09, 269.18 and 311.27. Following  $MS^4$ , the sample amounts are low; so in further studies only highly abundant ions were considered in structure analysis. Through  $MS^n$  analyses, the fragmentation patterns of  $m/z$  373.18 in the  $MS^2$  spectrum of ion  $m/z$  477 and the ion  $m/z$  343.18 in the  $MS^2$  spectrum of peak 373.18 were obtained (Fig. 2.14 and 2.15). From these studies, the fragment,  $m/z$  373.18 in the  $MS^2$  spectrum of peak 477 may be considered a marker ion for trehalose.

In the  $MS^2$  spectrum of ion  $m/z$  477 of permethylated trehalose standard, the ion with  $m/z$  403.18 is one of the major peaks. Its further fragmentation is also studied by ESI mass spectrometer (Fig. 2.16). Three major peaks have been found as: 257.09, 259.18 and 373.18. The structure and fragmentation pattern of this  $m/z$  403.18 ion is showed (Fig. 2.17).

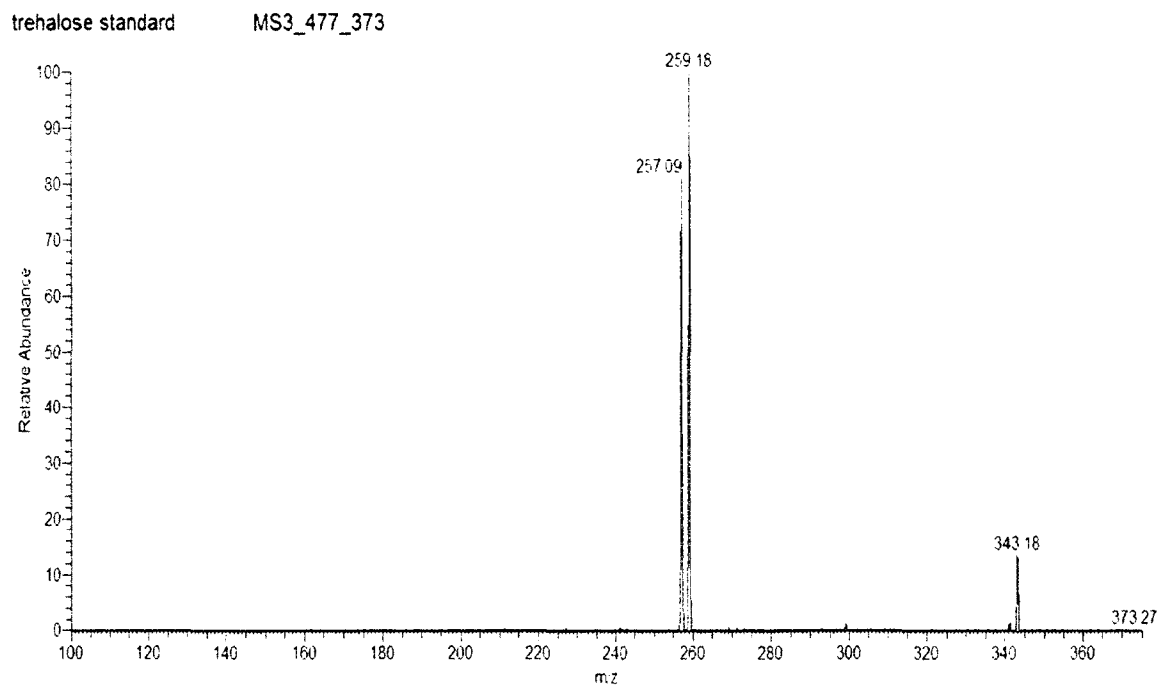


Fig. 2.12 MS<sup>3</sup> m/z 477-373 of permethylated trehalose standard 0.0342 $\mu$ g/ $\mu$ l

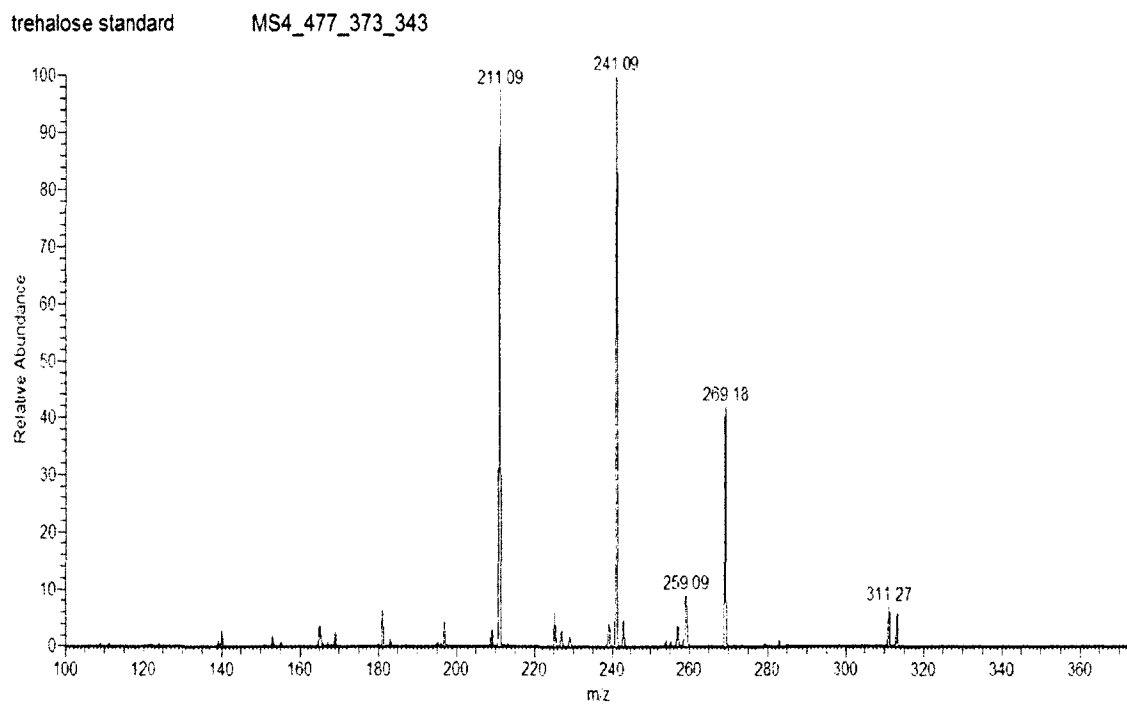


Fig. 2.13 MS<sup>4</sup> m/z 477-373-343 of permethylated trehalose standard 0.0342 $\mu$ g/ $\mu$ l



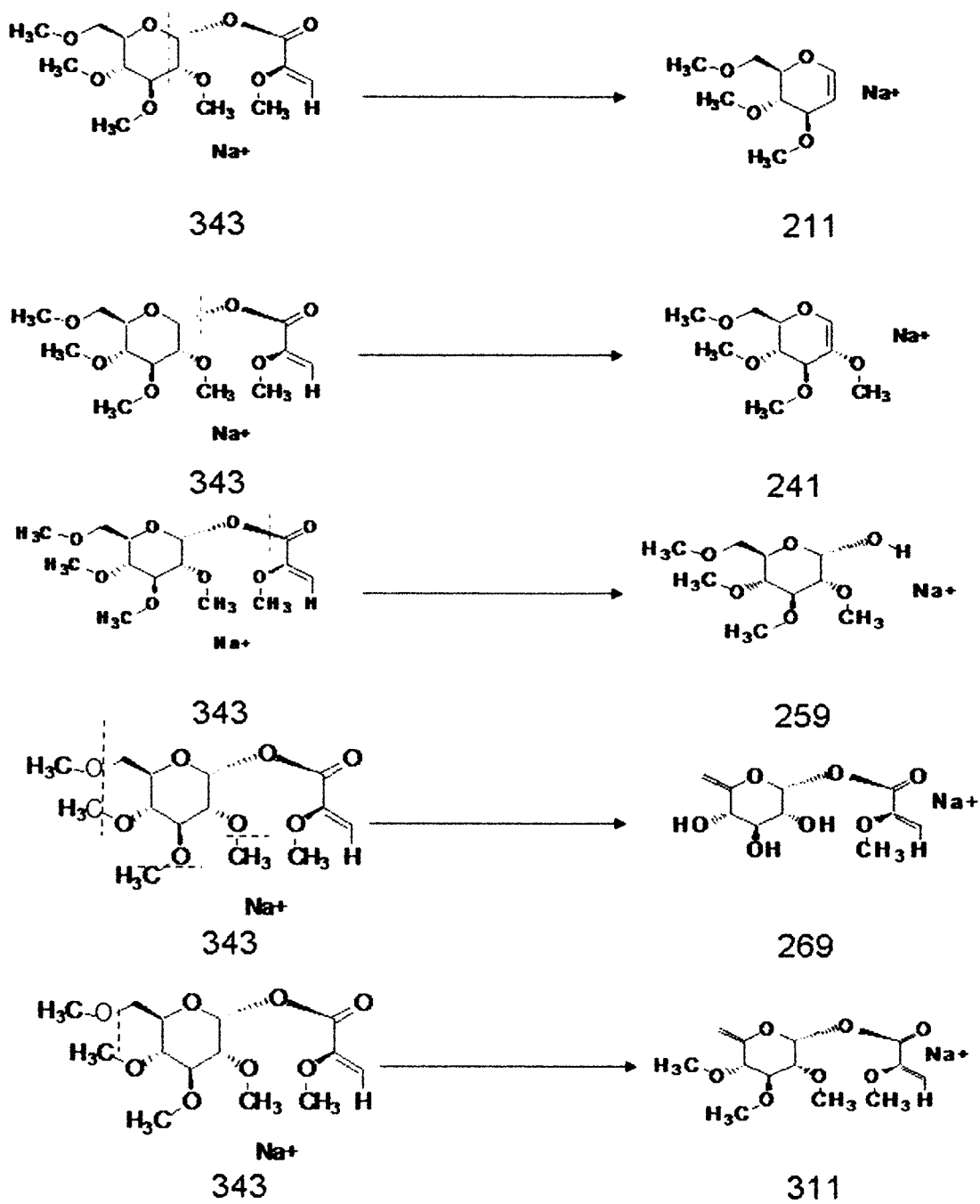


Fig. 2.15 Fragmentation patterns proposed for product ions of MS<sup>4</sup> m/z 477-373-343 of permethylated trehalose standard 0.0342µg/µl

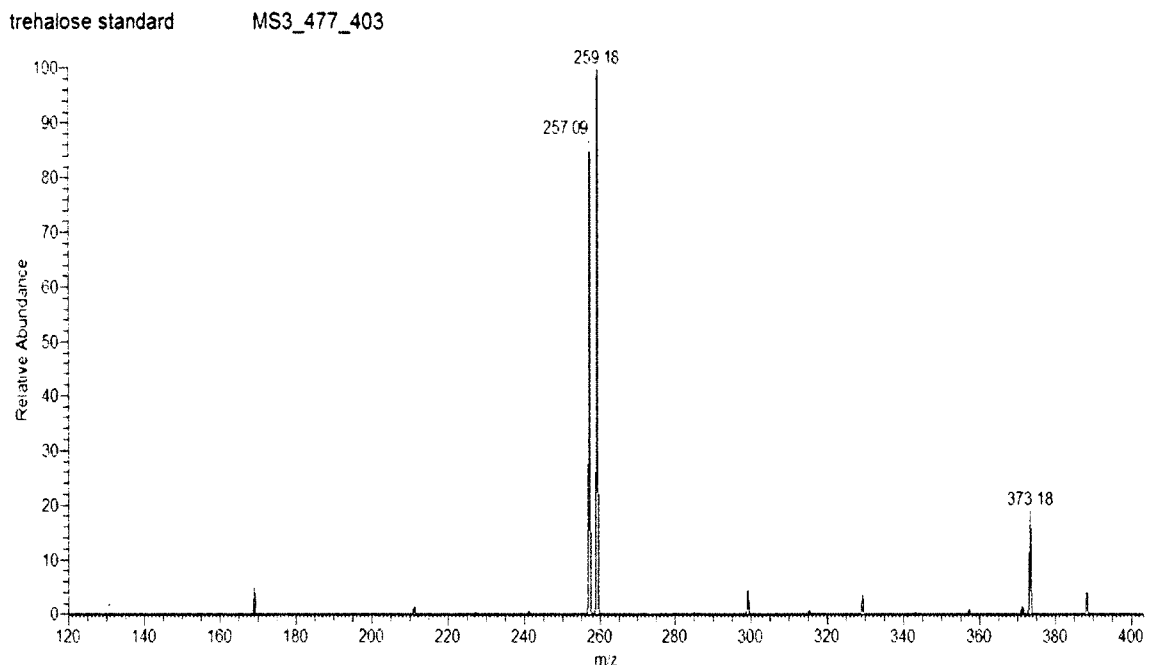


Fig. 2.16 MS<sup>3</sup> m/z 477-403 of permethylated trehalose standard 0.0342 $\mu$ g/ $\mu$ l

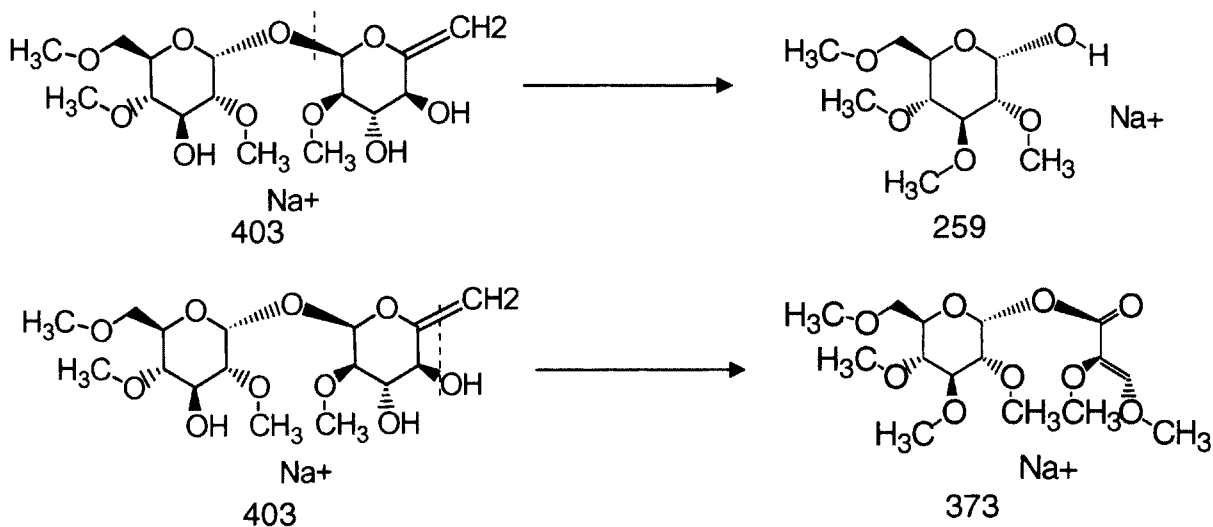
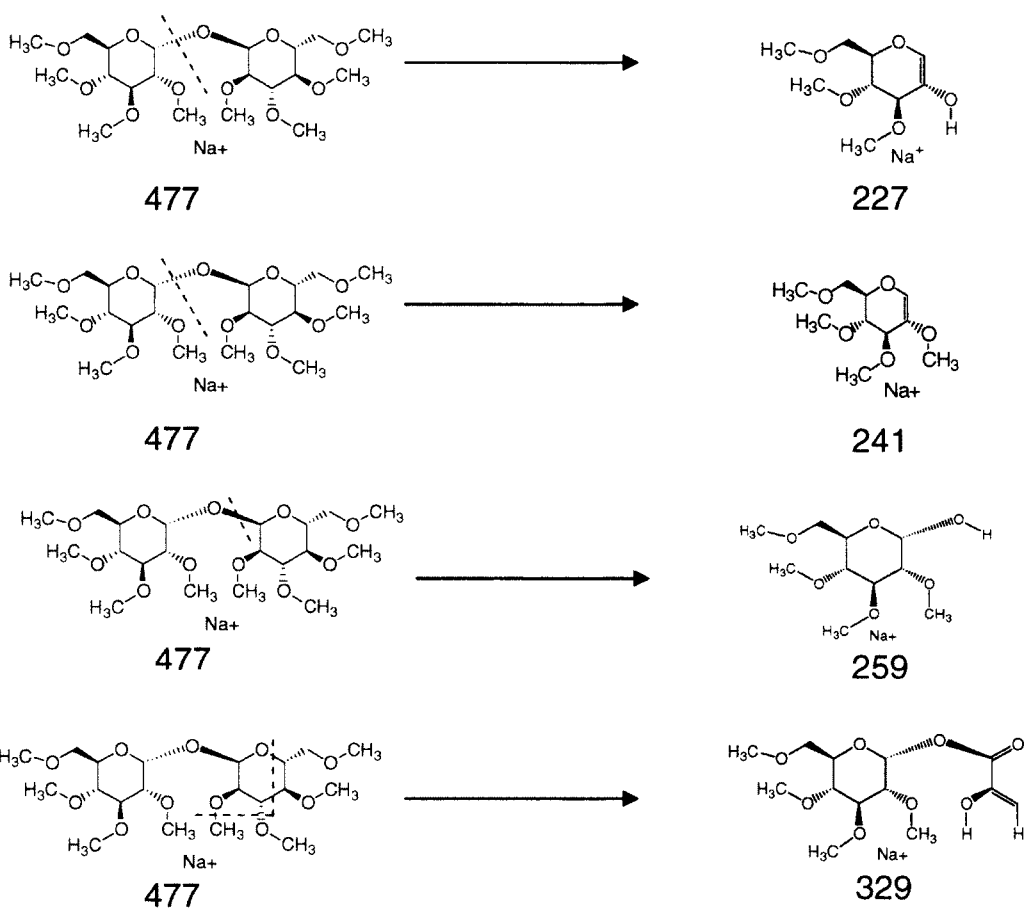
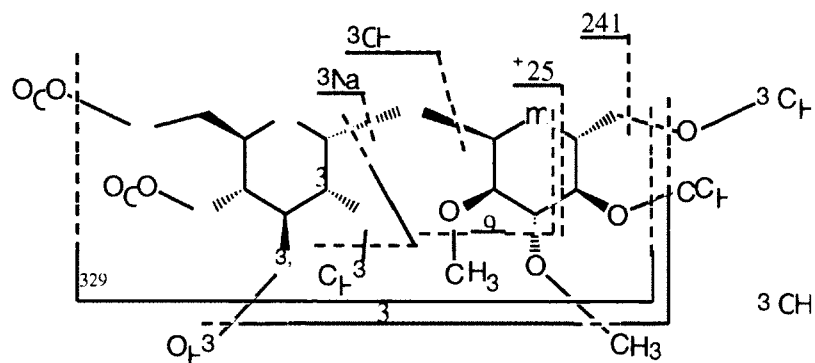


Fig. 2.17 Fragmentation patterns proposed for the product ions of MS<sup>3</sup> m/z 477-403 of permethylated trehalose standard 0.0342 $\mu$ g/ $\mu$ l





From the results above, the fragmentation patterns (Fig. 2.18) of permethylated trehalose standard has been obtained which can be used as a

standard to compare with *Porphyra* extracts samples. Although sequential mass spectrometry has been used in studying trehalose and has been published in many research papers<sup>37, 38, 39</sup>, it is the first time that the fragmentation pattern of permethylated trehalose has been studied. Since the standard fragmentation patterns of trehalose has been elucidated, the next step will be to compare the MS<sup>n</sup> of the *Porphyra* samples with that of the trehalose standard to find out if trehalose indeed exists in the *Porphyra* extracts.

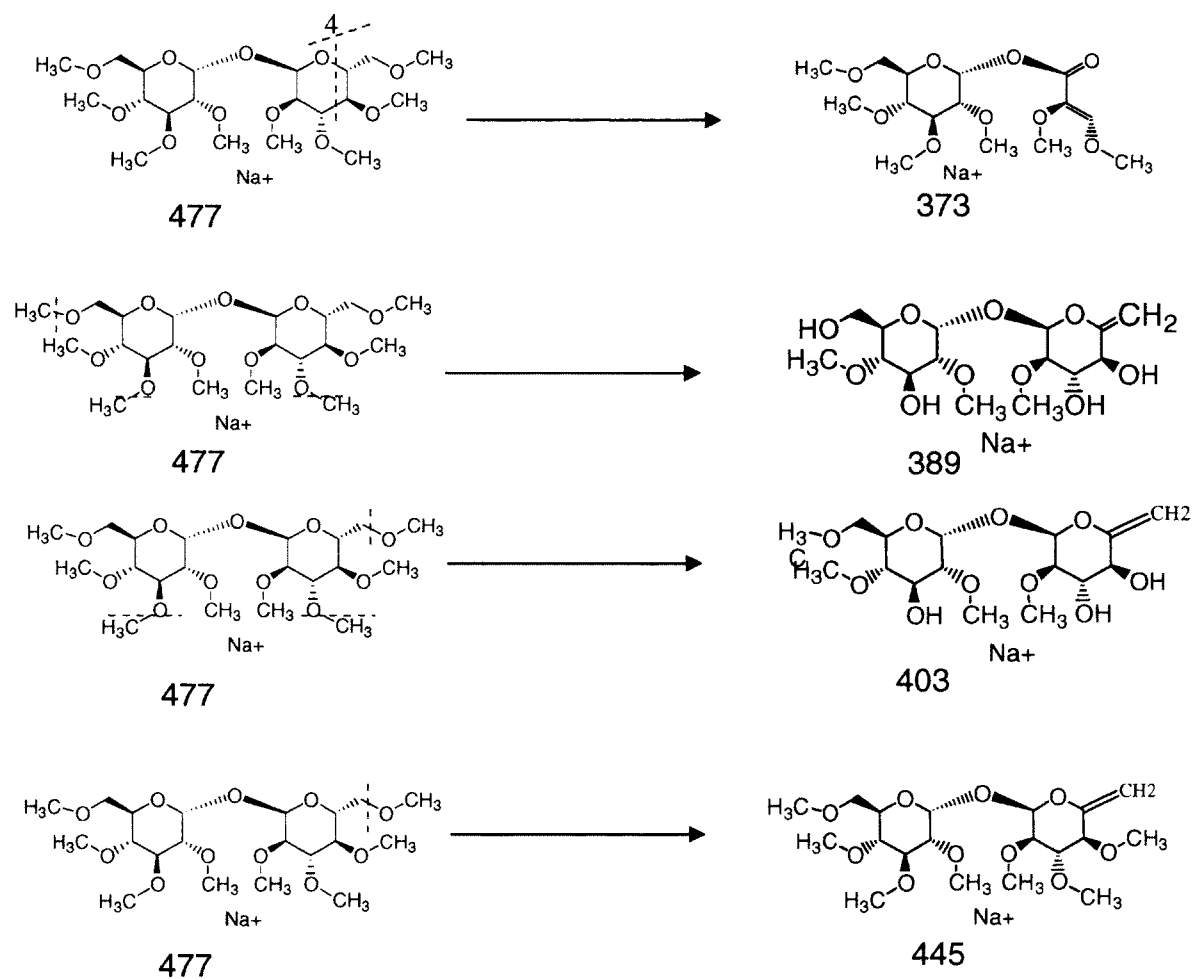


Fig. 2.18 Fragmentation patterns proposed for permethylated trehalose

### **(3) Comparison of MS<sup>n</sup> of peak 477**

MS<sup>n</sup> of ions m/z 477 from the Porphyra extracts samples have been studied and their comparison of the MS<sup>2</sup> m/z 477 with that from the fully hydrated Porphyra extracts, fully hydrated Porphyra extracts with 3.42µg trehalose standard added as the internal standard, and the partially desiccated Porphyra extracts are compiled (Fig. 2.19). All four samples have very similar MS<sup>2</sup> spectra (Table 2.2).

	Trehalose standard 3.42µg	Fully hydrated Porphyra extracts	Fully hydrated Porphyra extracts with trehalose standard 3.42µg	Partially desiccated Porphyra extracts
227	√	√	√	√
241	√	√	√	√
259	√	√	√	√
329	√	√	√	√
373	√	√	√	√
389	√	√	√	√
403	√	√	√	√
445	√	√	√	√

Table 2.2 major peaks in the MS<sup>2</sup> of ion m/z 477 of permethylated samples: trehalose standard 0.0342µg/µl; fully hydrated Porphyra extracts; fully hydrated Porphyra extracts with trehalose standard 0.0342µg/µl; partially desiccated Porphyra extracts.

All major peaks have been labeled with a red line. The only difference between Porphyra extracts samples and trehalose standard is the ion with m/z 347 peak which shows up as a major peak in Porphyra extracts samples while as

a minor peak in trehalose standard. MS<sup>2</sup> was conducted to study it deeply in trehalose standard sample but no more information could be obtained from the MS<sup>2</sup> which is probably because the amount of it is too low to be detected by LTQ mass spectrometer.

In order to confirm whether it is trehalose that exist in Porphyra extracts samples, further disassembly was carried out the higher abundance products m/z 477, including m/z 241 (Fig. 2.20), m/z 259 (Fig. 2.21), m/z 373 (Fig. 2.22), and m/z 403 (Fig. 2.23). From the MS<sup>3</sup> spectra m/z 477\_241 comparison of the permethylated samples, the four samples have exactly the same set of major peaks. There was a small difference between the Porphyra extracts samples and the trehalose standard (m/z 153) that shows up as a major peak in Porphyra extracts samples while only as a minor peak in the trehalose standard. In the comparison of MS<sup>3</sup> m/z 477\_259, the four samples also have the same set of peaks while the difference between them is that there is more background noise peaks in the Porphyra extracts samples which may be expected because these extracts cannot be as pure as the commercial trehalose standard sample. Comparison of MS<sup>3</sup> m/z 477\_373 from four samples showed that they are exactly the same, with the same set of ions and relative abundance. From the comparison of MS<sup>3</sup> m/z 477\_373 of the four permethylated samples, the same set of peaks have been obtained except the Porphyra samples have more background noise peaks due to the same reason mentioned above. From these data, we can conclude that we are able to detect trehalose in the Porphyra extracts samples. This is the first time that trehalose is definitively identified in

Porphyra extracts and it is also the first time that sequential mass spectrometry is used in studying Porphyra.

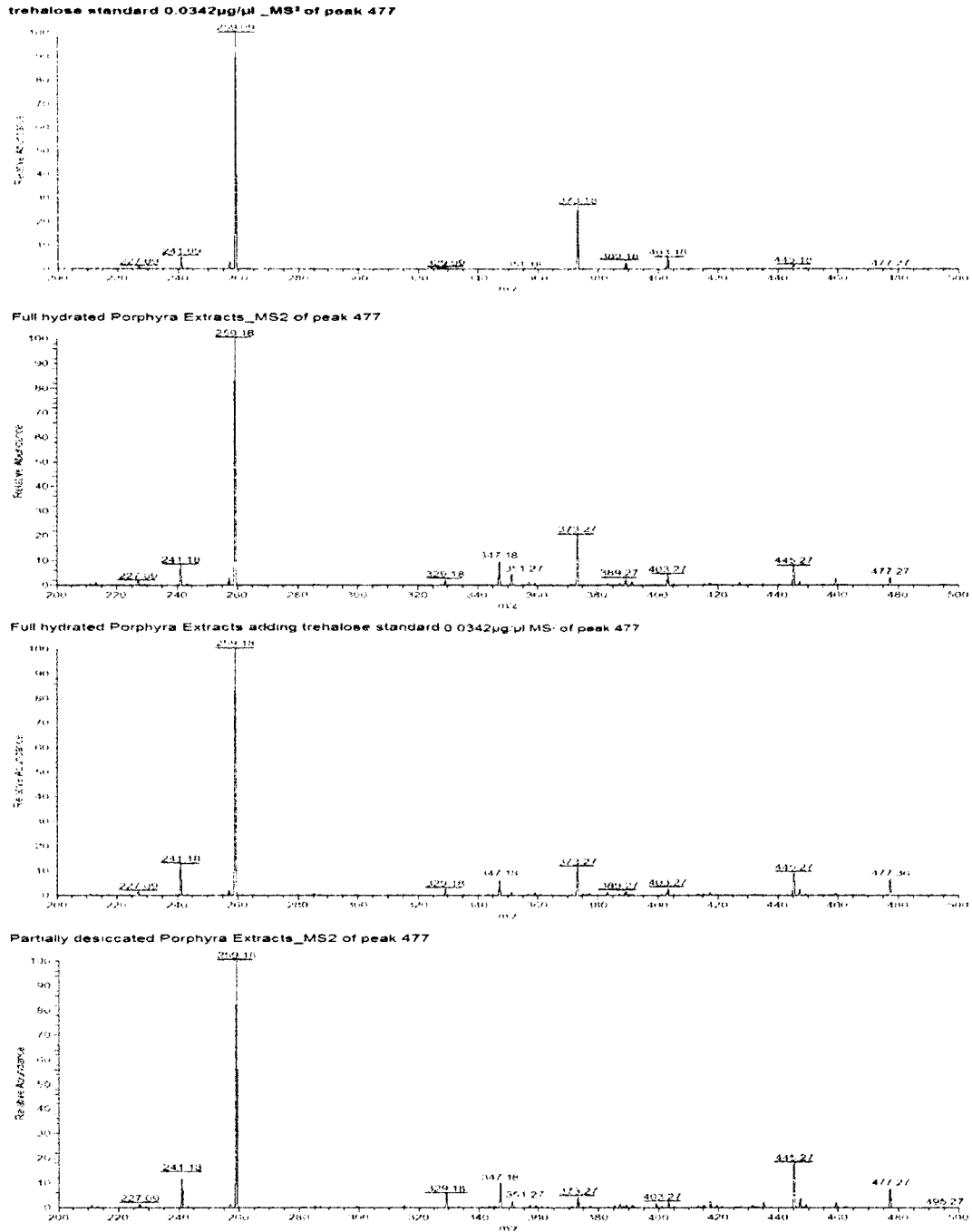


Fig. 2.19 MS<sup>2</sup> of ion m/z 477 of permethylated samples: trehalose standard 0.0342µg/µl; fully hydrated Porphyra extracts; fully hydrated Porphyra extracts with trehalose standard 0.0342µg/µl added as the internal control; partially desiccated Porphyra extracts.

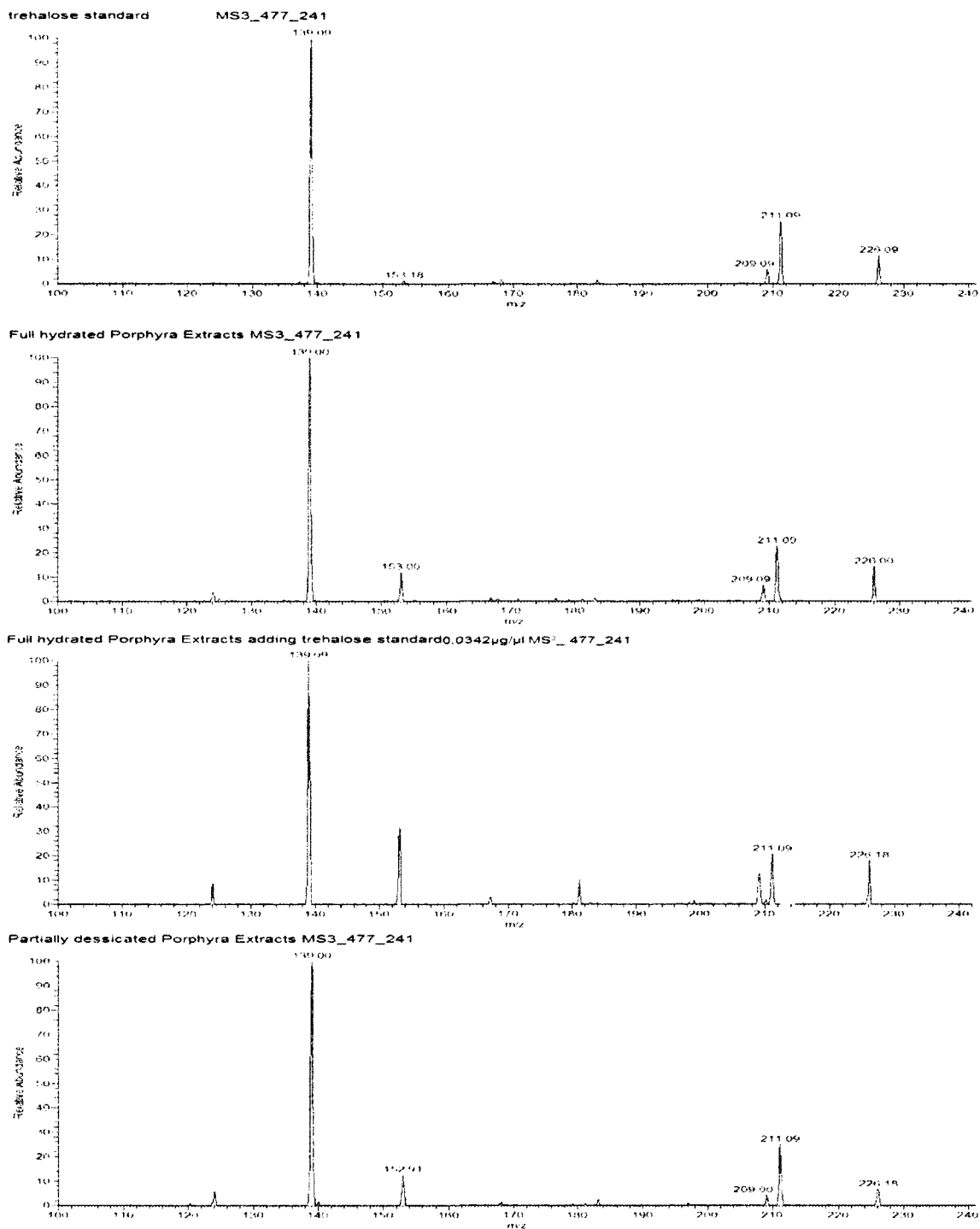


Fig. 2.20 MS<sup>3</sup> m/z 477\_241 of permethylated samples: trehalose standard 0.0342µg/µl; fully hydrated Porphyra extracts; fully hydrated Porphyra extracts with trehalose standard 0.0342µg/µl added as the internal control; partially desiccated Porphyra extracts.

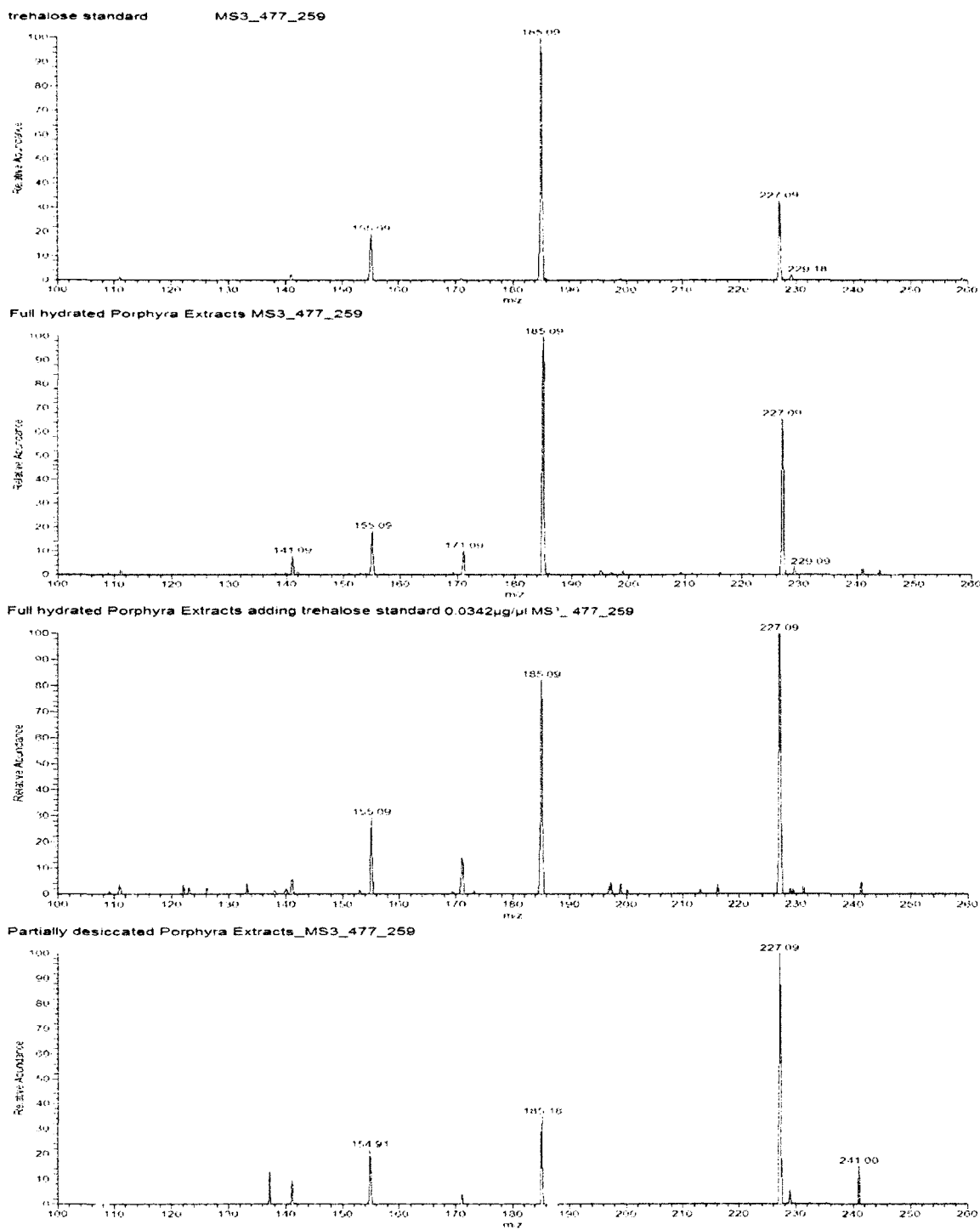


Fig. 2.21 MS<sup>3</sup> m/z 477\_259 of permethylated samples: trehalose standard 0.0342µg/µl; fully hydrated Porphyra extracts; fully hydrated Porphyra extracts with trehalose standard 0.0342µg/µl added as the internal control; partially desiccated Porphyra extracts.



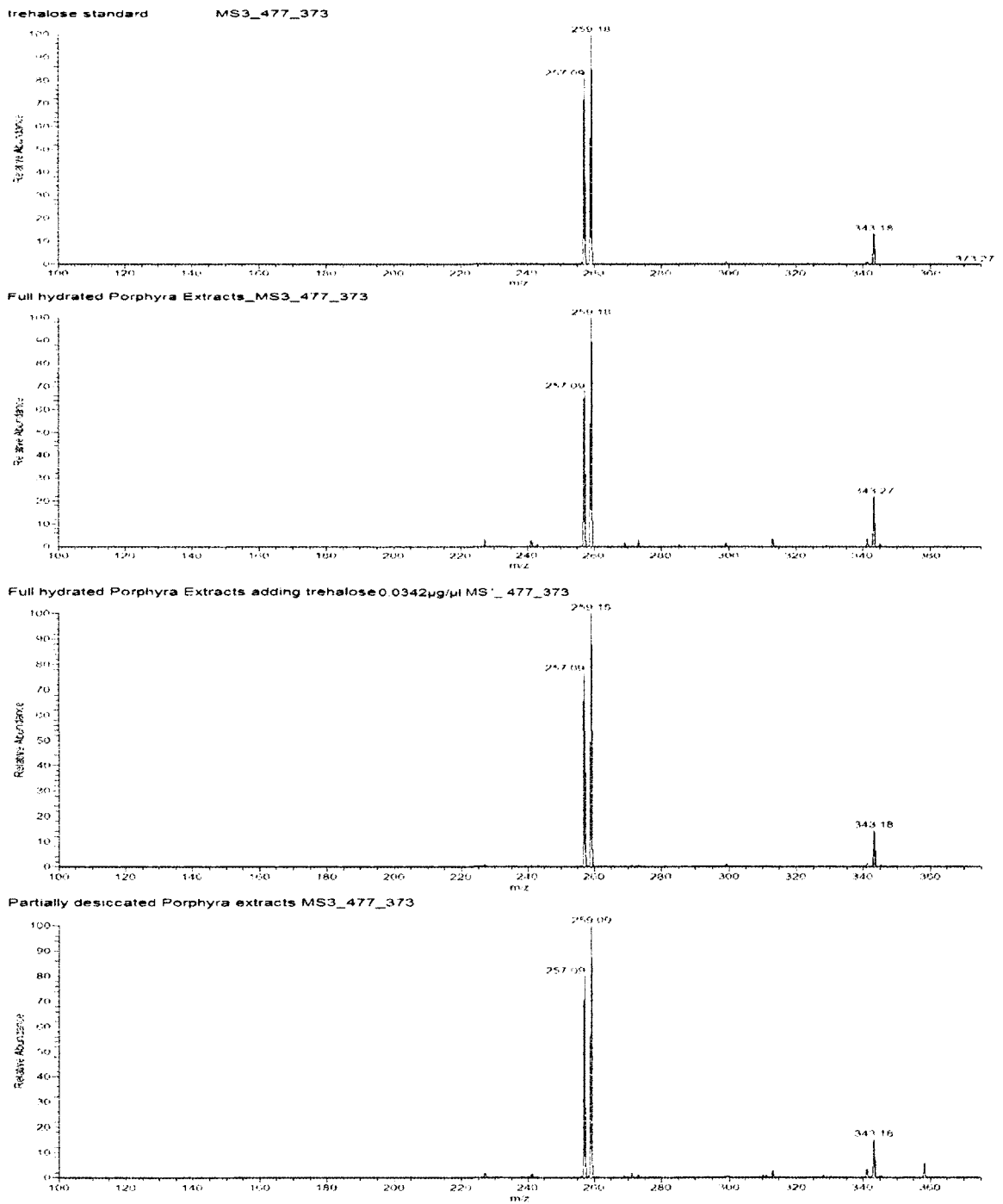


Fig. 2.22 MS<sup>3</sup> m/z 477\_373 comparison of permethylated samples: trehalose standard 0.0342µg/µl; fully hydrated Porphyra extracts; fully hydrated Porphyra extracts with trehalose standard 0.0342µg/µl added as the internal control; partially desiccated Porphyra extracts.

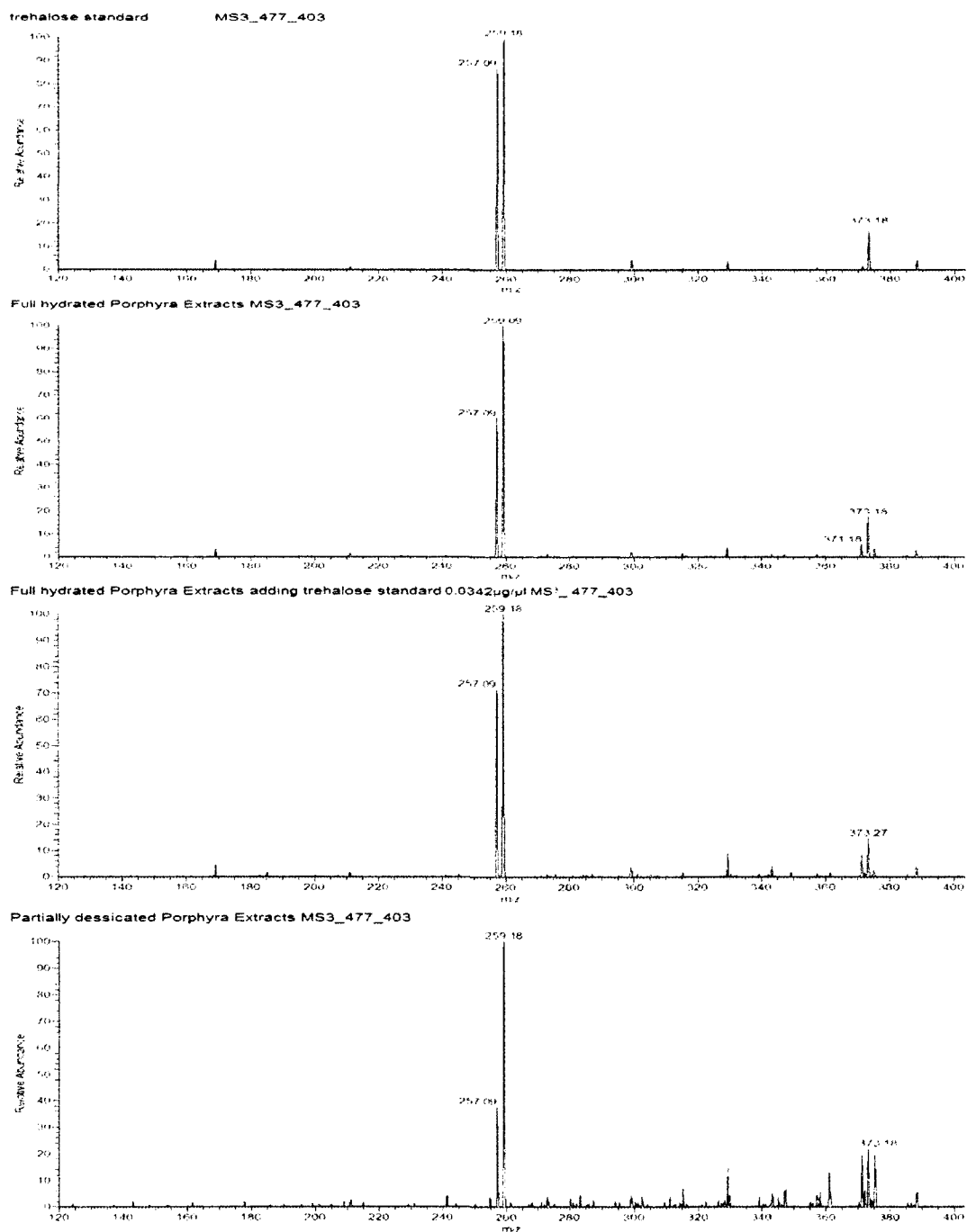


Fig. 2.23 MS<sup>3</sup> ion m/z 477\_403 of permethylated samples: trehalose standard 0.0342µg/µl; fully hydrated Porphyra extracts; fully hydrated Porphyra extracts with trehalose standard 0.0342µg/µl added as the internal control; partially desiccated Porphyra extracts.

## **Gas chromatography-mass spectrometry analysis**

Seven samples were processed in parallel and they are: ① the Blank sample, as the negative control; ② the sucrose standard 0.684 $\mu$ g; ③ the trehalose standard 0.684 $\mu$ g, in order to see the standard GC/MS chromatogram of trehalose; ④ a mixture of sucrose standard 0.684 $\mu$ g and trehalose standard 0.684 $\mu$ g; ⑤ the fully hydrated Porphyra extracts; ⑥ the fully hydrated Porphyra extracts with trehalose standard 0.684 $\mu$ g added into it as the internal control; ⑦ the partially desiccated Porphyra extracts. All of the samples were purified with PGC first and then prepared as TMS derivatives before they were injected into gas chromatography-mass spectrometer for analysis.

Although GC/MS has been widely used in trehalose detection and has been reported many times<sup>43, 45 and 46</sup>, different groups use different GC columns and, when the same type of column is used, different temperature programs were used. So first of all, we need to make sure our GC program is appropriate. Sucrose is the other non-reducing disaccharide that has been found so far, which has the same molecular weight as trehalose. The GC chromatograms of sucrose, trehalose, and a mixture of sucrose and trehalose of the same amount show that our GC method had resolving ability to separate and detect trehalose (Fig. 2.24). The retention time of trehalose is 9.31 min, while it is 8.52 min for sucrose (Table 2.3). The difference between the retention time of the same saccharide in the single and the

mixed samples is very small; for trehalose the retention time is exactly the same suggesting reliability.

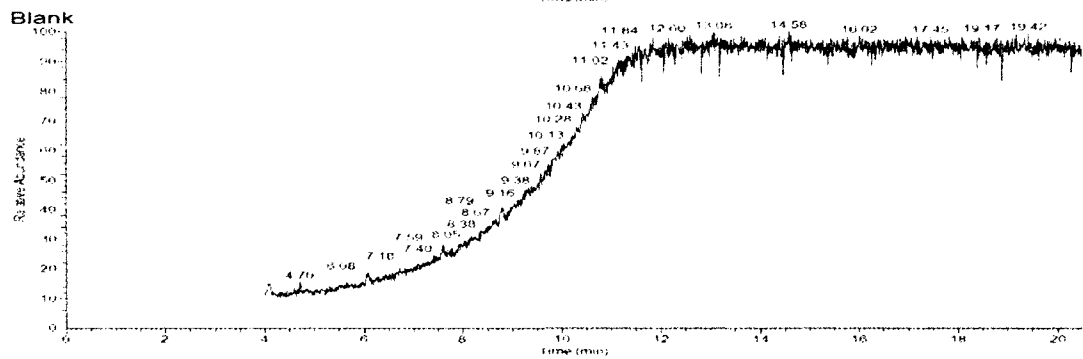
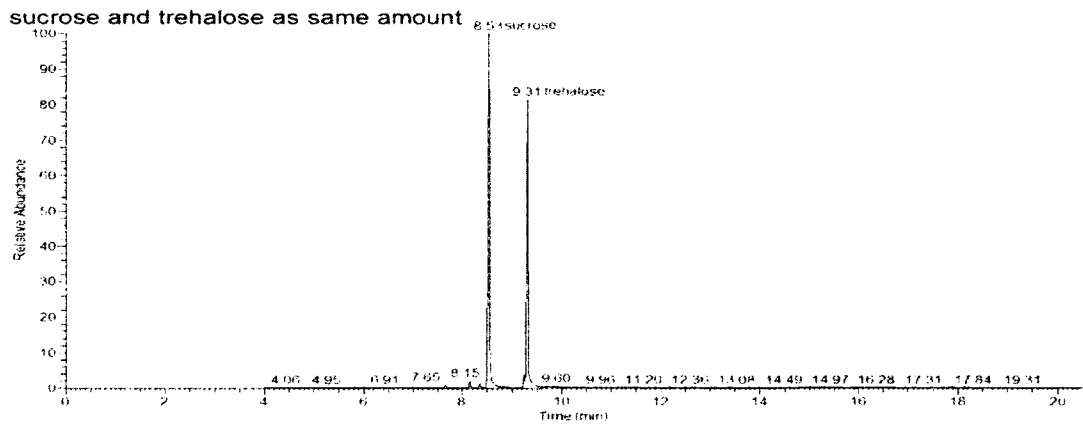
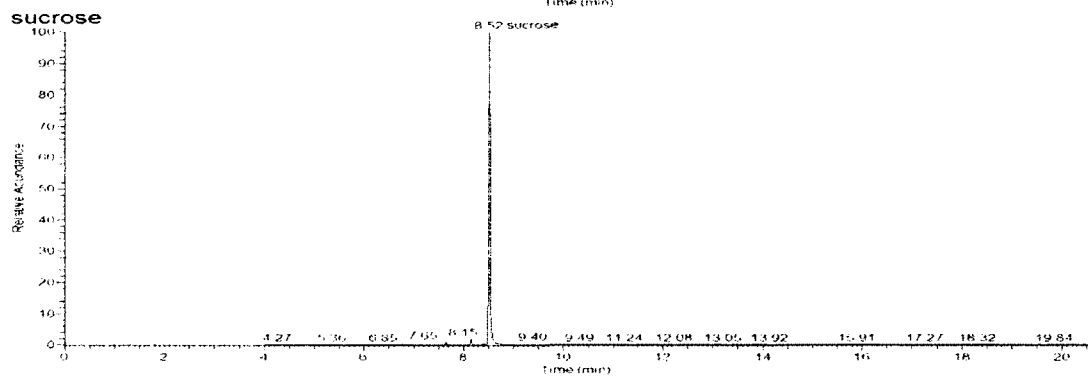
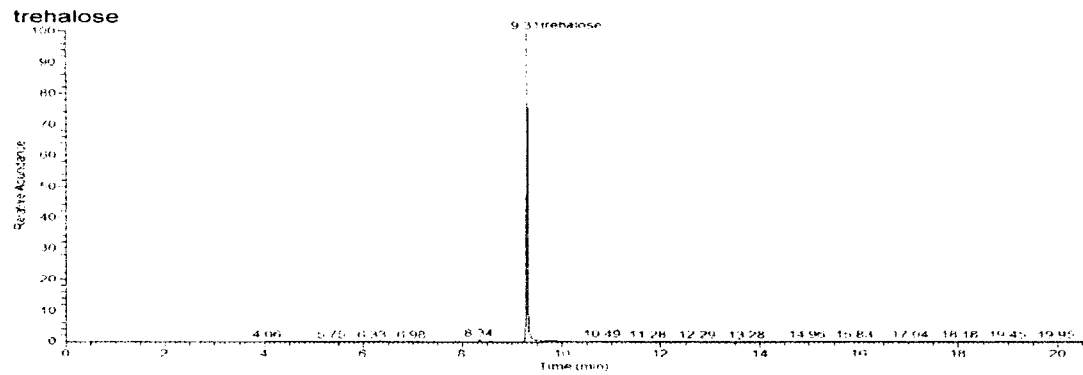


Fig. 2.24 GC chromatogram of trehalose

	Retention time of single saccharide (min)	Retention time of mixed saccharide (min)	Time difference (min)
Trehalose	9.31	9.31	0.00
Sucrose	8.52	8.53	0.01

Table 2.3 Comparison of characteristic peak retention time on carbohydrate derivative

Five concentrations of trehalose standard solution were prepared to generate a standard curve for quantitative analysis. They are 0 pmol, 5000 pmol, 10000 pmol, 15000 pmol and 20000 pmol. These five samples are processed in parallel and dried out before the preparation of TMS derivatives and then they were injected into the gas chromatography-mass spectrometer for quantitative analysis, (Table 2.4). This was repeated three times and the peak area were average. Using Microsoft Excel, we calculated the relationship between the characteristic peak area of trehalose and the quantity of trehalose as  $Y=1034X+1534.1$ , Y is the amount (pmol) of trehalose and X is the characteristic peak area of trehalose derivative,  $R^2$  is 0.9752 (Fig. 2.25). This standard curve will be used in the quantification of trehalose in the Porphyra extracts samples.

Trehalose standard	A	B	C	D	E
pmol	0	5000	10000	15000	20000
Peak area ( $E^4$ )	0	1.71	3.42	5.13	6.84

Table 2.4 The relation of trehalose derivative characteristic peak area and trehalose quality

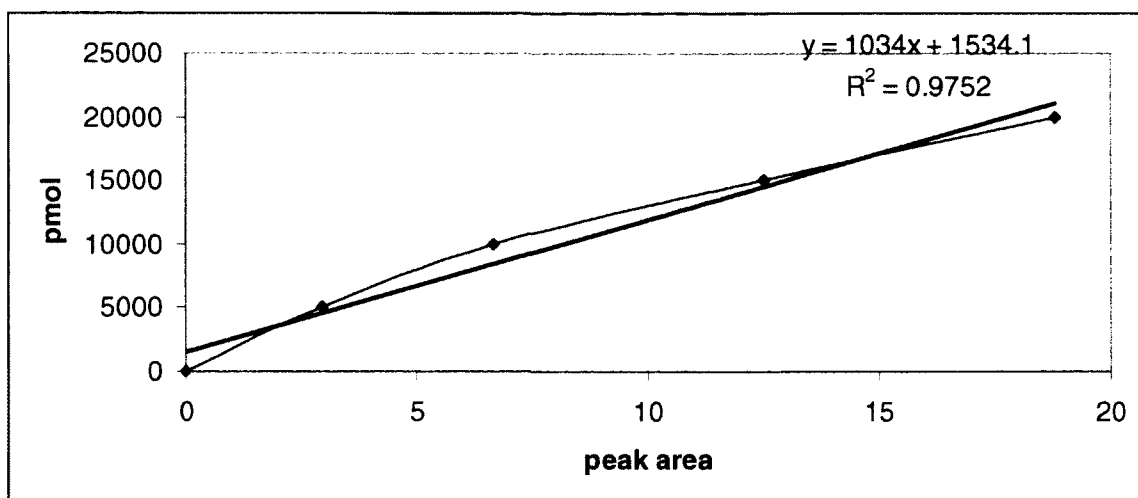


Fig. 2.25 Standard curve of trehalose quantification using GC; The amount of trehalose was plotted against the characteristic peak area in the GC chromatograms

The trehalose standard 0.684 $\mu$ g, the fully hydrated *Porphyra* extracts, the fully hydrated *Porphyra* extracts with trehalose standard 0.684 $\mu$ g and the partially desiccated *Porphyra* extracts were processed in parallel. They were purified with PGC first and then prepared as TMS derivatives before they were finally injected into the gas chromatography-mass spectrometer for analysis. In the GC chromatograms of *Porphyra* extracts (Fig. 2.26), we found a peak at the retention time of 9.27min, which is 0.04min different from that of the standard trehalose samples. Especially, in the chromatogram of the fully hydrated *Porphyra* extracts with trehalose standard 6.84 $\mu$ g added, the peak area at 9.27min increases significantly, and it is the only peak that increases after 6.84 $\mu$ g of trehalose standard is added into the fully hydrated *Porphyra* extracts, which suggests that this peak must be due to the existence of trehalose in the samples. Since this peak

exists in the chromatograms of all the Porphyra extracts samples, it suggests trehalose must exist in the Porphyra.

We also compared the mass spectra of the 9.27min peak in the GC chromatograms of the trehalose standard and the Porphyra extracts samples (Fig. 2.27); they are essentially the same. This also suggests that trehalose does exist in the Porphyra extracts.

Next, we quantified the amount of trehalose in the different Porphyra extracts samples using the standard curve developed above. The experiments were repeated three times and the average peak area were calculated. As a result, there is 7133 pmol trehalose in the fully hydrated Porphyra extracts and 5762 pmol trehalose in the partially desiccated Porphyra extracts (Table 2.5). Since the weight of each Porphyra extracts sample is 60mg, every 10mg of fully hydrated Porphyra extracts contain 0.4066 $\mu$ g of trehalose and every 10mg of partially desiccated Porphyra extracts have 0.3284 $\mu$ g of trehalose. Therefore, it seems that there is a smaller amount of trehalose in the partially desiccated Porphyra. We currently do not understand why this is the case. Further study is surely needed to understand why the amount of trehalose decreases after it is subject to desiccation and how trehalose helps Porphyra survive during desiccation.

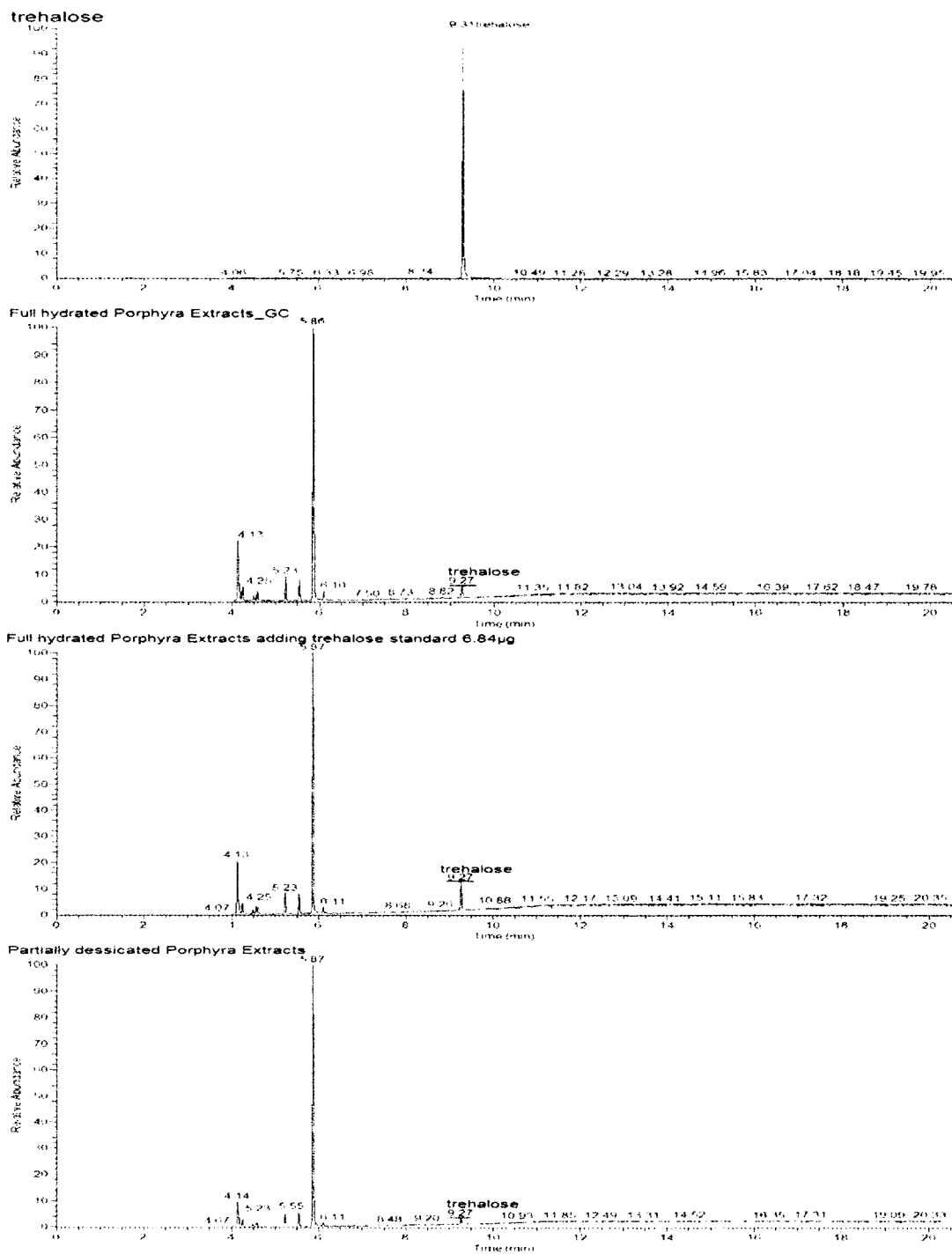


Fig. 2.26 GC chromatograms of the trehalose standard 0.684µg, the fully hydrated Porphyra extracts, the fully hydrated Porphyra extracts with trehalose standard 0.684µg added into it as the internal control and the partially desiccated Porphyra extracts



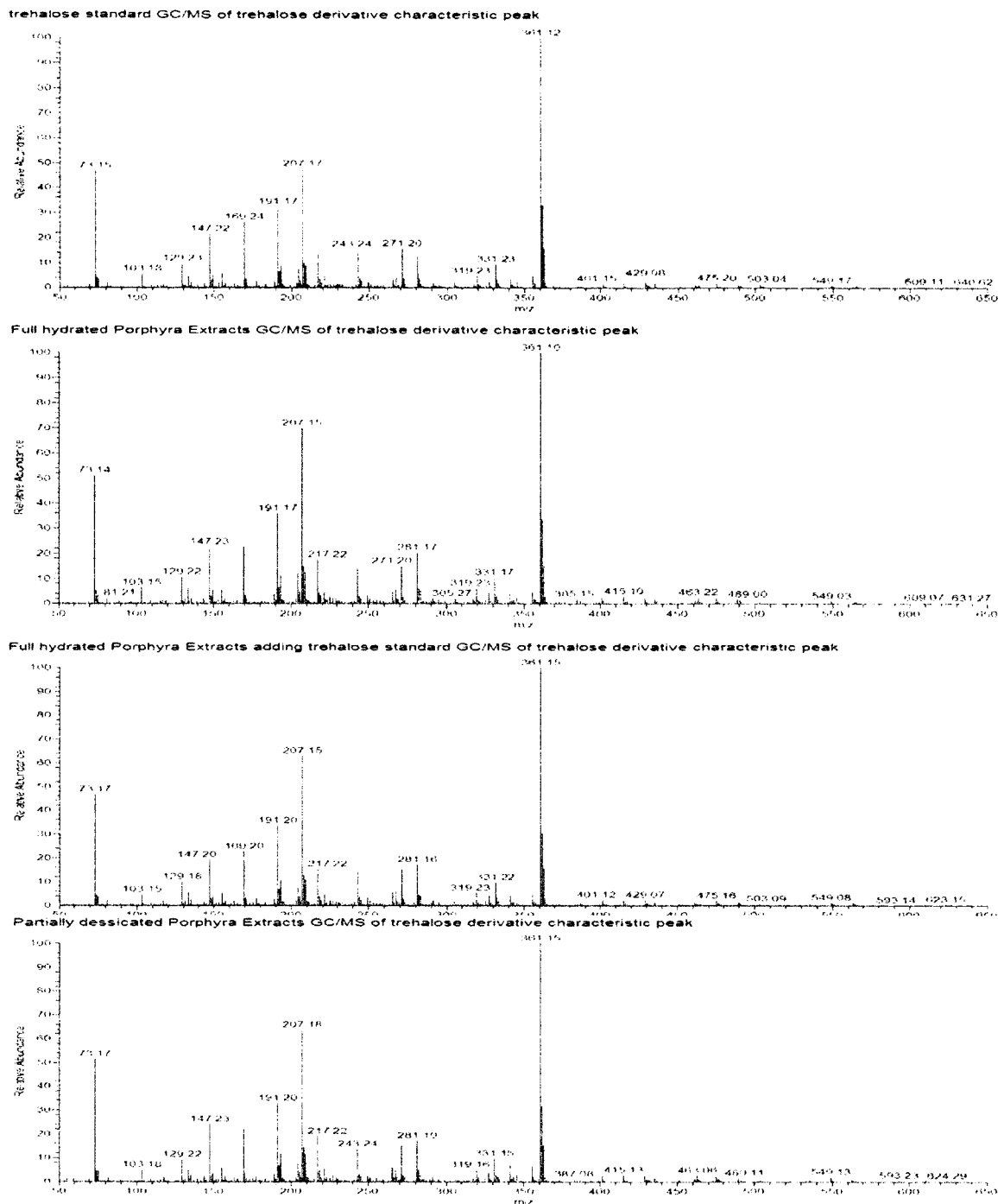


Fig. 2.27 GC/MS comparison of trehalose derivative characteristic peak of the trehalose standard 0.684 $\mu$ g, the fully hydrated Porphyra extracts, the fully hydrated Porphyra extracts with trehalose standard 0.684 $\mu$ g added into it as the internal control and the partially desiccated Porphyra extracts

Porphyra extracts	Peak area	Trehalose amount (pmol)	Every 10mg Porphyra extracts containing trehalose ( $\mu\text{g}$ )
Fully hydrated	5.36	7133	0.4066
Partially desiccated	4.05	5762	0.3284

Table 2.5 Comparison of trehalose content between full hydrated and partially desiccated Porphyra extracts

## **2.4 Conclusions**

We were able to detect trehalose in Porphyra extracts for the first time and thus authenticate the existence of trehalose in this plant, which has been speculated in the field of seaweed study for a long time<sup>40, 41, and 42</sup>.

We have demonstrated that trehalose can be effectively detected in Porphyra extracts using mass spectrometry and especially by using ion trap mass spectrometry coupled with sequential disassembly. This is also the first time that the fragmentation patterns of permethylated trehalose have ever been obtained and it can serve as a standard for others to compare and improve. Our results suggest that sequential mass spectrometry, coupled with appropriate sample preparation and data interpretation techniques, can be an ideal way to detect carbohydrates in plant extracts samples.

Although GC/MS has been routinely used to detect and analyze trehalose from other sources, this is the first time it has successfully detected trehalose from Porphyra extracts.

## REFERENCES

1. David L. Nelson; Michael M. Cox. 2005. *Lehninger Principles of Biochemistry*, 4th edition.
2. Varki, Ajit; Cummings, Richard; Esko, Jeffrey; Freeze, Hudson; Hart, Gerald; Marth, Jamey, editors. 1999. Plainview, Cold Spring Harbor Laboratory Press.
3. Varki, A.; Cummings, R.D.; Esko, J.D.; Freeze, H.H.; Stanley, P.; Bertozzi, C.R.; Hart, G.W.; Etzler, M.E. 2008. *Essentials of Glycobiology* 2nd edition.
4. Varki A. 1993. Biological roles of oligosaccharides: All of the theories are correct. *Glycobiology* 3: 97–130.
5. Jiao, Hongqin; Zhang, Hailong; Reinhold, Vernon N. 2011. High Performance IT-MSn Sequencing of Glycans (Spatial Resolution of Ovalbumin Isomers). *Int. J. of Mass Spectrometry* 303:109–117.
6. Apweiler R, Hermjakob H, Sharon N.1999. On the frequency of protein glycosylation, as deduced from analysis of the SWISS-PROT database. *Biochim Biophys Acta* 1473: 4–8.
7. R. Kornfeld and S. Kornfeld. 1985. Assembly of asparagine-linked oligosaccharides. *Annu. Rev. Biochem.* 54: 631–634.
8. Stanley P. 1984. Glycosylation mutants of animal cells. *Annu Rev Genet.* 18: 525–552.
9. Freeze HH. 2006. Genetic defects in the human glycome. *Nat Rev Genet.* 7: 537–551.
10. Kamerling J, Boons G-J, Lee Y. 2007. *Comprehensive glycoscience.* 4. 339–372.
11. Justin M. Prien, Leanne C. Huysentruyt, David J. Ashline, Anthony J. Lapadula, Thomas N. Seyfried, and Vernon N. Reinhold. 2009. Differentiating N-linked glycan structural isomers in metastatic and nonmetastatic tumor cells using sequential mass spectrometry *J Am Soc Mass Spectrom, Glycobiology* 5: 353–366.
12. Vernon Reinhold, David J. Ashline, Hailong Zhang. 2010. Unraveling the Structural Details of the Glycoproteome by ITMS. Book chapter in *Practical Aspects of Trapped Ion Mass Spectrometry* (March RE & Todd JF, Eds.). CRC Press, pp.705-736.

13. Clowers BH, Hill HH Jr. 2005. Mass analysis of mobility-selected ion populations using dual gate, ion mobility, quadrupole ion trap mass spectrometry. *Anal Chem* 77(18):5877-85.
14. Ashline, D.; Singh, S.; Hanneman, A.; Reinhold, V. 2005. Congruent Strategies for Carbohydrate Sequencing.1. Mining Structural Details by MSn. *Anal. Chem.* 77, 6250-6262.
15. Zhang, H.; Singh, S.; Reinhold, V. 2005. Congruent strategies for carbohydrate sequencing. 2. FragLib: an MSn spectral library. *Anal. Chem.* 77, 6263-6270.
16. Lapadula, A.; Hatcher, P.; Hanneman, A.; Ashline, D.; Zhang, H.; Reinhold, V. 2005. Congruent strategies for carbohydrate sequencing. 3. OSCAR: an algorithm for assigning oligosaccharide topology from MSn data. *Anal. Chem.* 77, 6271-6279.
17. Justin M. Prien, David J. Ashline, Anthony J. Lapadula, Hailong Zhang, Vernon N. Reinhold; 2009. The high mannose glycans from bovine ribonuclease B isomer characterization by ion trap MS. *J Am Soc Mass Spectrom*, 20(4):539-56.
18. Brodie, J.A. and Irvine, L.M. 2003. Seaweeds of the British Isles. Volume Part 3b. The Natural History Museum, London. ISBN1898298874.
19. Hardy, F.G. and Guiry, M.D. 2006. A Check-list and Atlas of the Seaweeds of Britain and Ireland. British Phycological Society, London. ISBN 390616635X.
20. Mumford, T.F. and Miura, A. 1988. *Porphyra as food: cultivation and economics. Algae and Human Affairs.* Cambridge University Press, Cambridge. ISBN 0-521-32115-8.
21. Abbott, Isabella A. 1989. *Algae and human affairs.* Cambridge University Press, Phycological Society of America. pp. 141. ISBN 9780521321150.
22. Aoki, Y. and Kamei, Y. 2006. Preparation of recombinant polysaccharide-degrading enzymes from the marine bacterium, *Pseudomonas* sp. ND137 for the production of protoplasts of *Porphyra yezoensis* *Eur. J. Phycol.* 41: 321 – 328.
23. Sapir, Liel; Harries, Daniel. 2011. Linking Trehalose Self-Association with Binary Aqueous Solution Equation of State. *J. Phys. Chem. B* 115: 624–634.

24. Sola-Penna M, Meyer-Fernandes JR. 1998. Stabilization against thermal inactivation promoted by sugars on enzyme structure and function: why is trehalose more effective than other sugars. *Archives of Biochemistry and Biophysics* 360 (1): 10–14.
25. ULF Karsten, Solvig Gors, Anja Eggert, John A. West. 2007. Trehalose, digeneaside, and floridoside in the Florideophyceae (Rhodophyta) – a reevaluation of its chemotaxonomic value. *Phycologia* Volume 46(2), 143-150.
26. Paul H. Yancey. 2005. Organic osmolytes as compatible, metabolic and counteracting cytoprotectants in high osmolality and other stresses. *The Journal of Experimental Biology* 208, 2819-2830.
27. Higashiyama, Takanobu. 2002. Novel functions and applications of trehalose. *Pure Appl. Chem.* 74 (7): 1263–1269.
28. Craigie J.S. 1974. Storage products. *Algal physiology and biochemistry*, pp.206-225. Blackwell Scientific Press, Oxford.
29. Dai Y.D., Zhao G., Jin S.X., Ji L.Y., De L.D., Man L.W., Wang B. 2004. Construction and characterization of a bacterial artificial chromosome library of marine macroalga *Porphyra yezoensis* (Rhodophyta). *Plant Molecular Biology Reporter* 22: 375-386.
30. M. P. M. Reddy, M. Affholder. 2002. Descriptive physical oceanography: State of the Art. Taylor and Francis. p. 249.
31. Richard Hubbard. 1893. *Boater's Bowditch: The Small Craft American Practical Navigator*. McGraw-Hill Professional. pp. 54.
32. Zs. Fuzfai, I. Boldizsar, I. Molnar-Perl. 2008. Characteristic fragmentation patterns of the trimethylsilyl and trimethylsilyl-oxime derivatives of various saccharides as obtained by gas chromatography coupled to ion-trap mass spectrometry. *Journal of Chromatography A*. 1177.183-189.
33. Costello, C. E., Contado-Miller, J. M., Cipollo, J. F. 2007. A glycomics platform for the analysis of permethylated oligosaccharide alditols. *J. Am. Soc. Mass Spectrom.* 18,1799 - 12.
34. Zhao, C, Xie, B., Chan, S. Y., Costello, C. E., O'Connor, P. B. 2008. Collisionally activated dissociation and electron capture dissociation provide complementary structural information for branched permethylated oligosaccharides. *J. Am. Soc. Mass Spectrom.* 19,138 - 150.

35. Douglas M. Sheeley and Vernon N. Reinhold. 1998. Structural Characterization of Carbohydrate Sequence, Linkage, and Branching in a Quadrupole Ion Trap Mass Spectrometer: Neutral Oligosaccharides and N-Linked Glycans *Anal. Chem.*, 1998, 70 (14), pp 3053–3059.
36. Domon, Bruno; Costello, Catherine E; 1988. A systematic nomenclature for carbohydrate fragmentations in FAB-MS/MS spectra of glycoconjugates. *Glyconjugate Journal*, Volume 5, 397-409.
37. Shin Muramoto, Jeremy Brison, David G. Castner. 2010. ToF-SIMS Depth Profiling of Trehalose: The Effect of Analysis Beam Dose on the Quality of Depth Profiles. *Volumn43*, Issue 1-2.
38. Elizabeth R. Rhoades, Cassandra Streeter, John Turk, and Fong-Fu Hsu. 2011. Characterization of sulfolipids of *Mycobacterium tuberculosis* H37Rv by multiple-stage linear ion-trap high-resolution mass spectrometry with electrospray ionization reveals that the family of sulfolipid II predominates. *50(42):9135-47*.
39. Kuni Takayama and Emma Lee Armstrong. 1976. Isolation, Characterization, and Function of 6-Mycolyl-6'-acetyltrehalose in the H 3 7Ra Strain of *Mycobacterium tuberculosis*. *Mycolylacetyltrehalose*. Volume 15, NO.2, pp 441-447.
40. Paul H. Yancey. 2005. Organic osmolytes as compatible, metabolic and counteracting cytoprotectants in high osmolarity and other stresses. *The Journal of Experimental Biology* 208, 2819-2830.
41. ULF Karsten, Dirk Michalik, Manfred Michalik and John A. West. 2005. A new unusual low molecular weight carbohydrate in the red algal genus *Hypoglossum* (Delesseriaceae, Ceramiales) and its possible function as an osmolyte. *Planta*, Volumn 222. 319-326.
42. Yancey, P. H., Rhea, M. D., Kemp, K. M. and Bailey, D. M. 2004. Trimethylamine oxide, betaine and other osmolytes in deep-sea animals: depth trends and effects on enzymes under hydrostatic pressure. *Cell. Mol. Biol.* 50, 371-376.
43. Zs. Fuzfai, I. Oldizsar, I. Molnar-Perl. 2008. Characteristic fragmentation patterns of the trimethylsilyl and trimethylsilyl-oxime derivatives of various saccharides as obtained by gas chromatography coupled to ion-trap mass spectrometry. *Journal of chromatography A*. 183-189.
44. Tohru Yamagaki, Kazuhiko Fukui, and Kazuo Tachibana. 2006. Analysis of Glycosyl Bond Cleavage and Related Isotope Effects in Collision-Induced Dissociation Quadrupole-Time-of-Flight Mass Spectrometry of Isomeric

Trehaloses. *Anal. Chem.* 2006, 78, 1015-1022.

45. Perline MI, Horvath K, Katona Z. 2000. The possibilities of GC/MS and HPLC in the analysis of sugars and acids in natural matrices. 70(3-6):231-8.
46. Jason P. Acker, Xiao-ming Lu, Vernon Young, Stephen Cheley, Hagan Bayley, Alex Fowler, Mehmet Toner. 2003. Measurement of Trehalose Loading of Mammalian Cells Porated With a Metal-Actuated Switchable Pore. *Biotechnology and bioengineering*, VOL. 82, NO. 5.